TU Munich, 16-20 September 2013, RB Summer School

An introduction to geometrical parametrizations for the applications of reduced order modelling: learning by examples

ADVANCES

Gianluigi Rozza,

Collaboration Network

MOX (A. Quarteroni, F. Ballarin, P. Pacciarini)

EPFL (T. Lassila, F. Negri, P. Chen, D. Forti)

MIT (A.T. Patera, D.B.P. Huynh, C.N. Nguyen)

SISSA (A. Manzoni, D. Devaud), U. Konstanz (L. Iapichino)

Reduction strategies for simulation/**optimization** of complex systems

Goal: to achieve the **accuracy** and **reliability** of a high fidelity approximation but at greatly **reduced cost** of a **low order model**

Forward and Inverse problems related with geometry/shape variation

- Shape changes make in general numerical simulations quite unaffordable, due to mesh deformations and domain-dependent FE structures assembling
- Iterative procedures (e.g. for shape optimization) require multiple evaluations of outputs depending on field variables and/or geometry

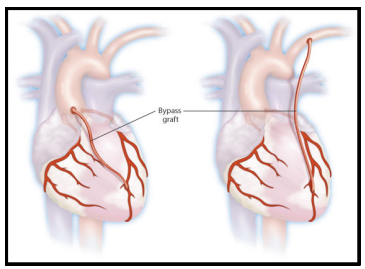

Reduction strategies for simulation/**optimization** of complex systems

Goal: to achieve the **accuracy** and **reliability** of a high fidelity approximation but at greatly **reduced cost** of a **low order model**

Forward and Inverse problems related with geometry/shape variation

- Shape changes make in general numerical simulations quite unaffordable, due to mesh deformations and domain-dependent FE structures assembling
- Iterative procedures (e.g. for shape optimization) require multiple evaluations of outputs depending on field variables and/or geometry

Way: coupling suitable **shape parametrizations** with **reduced basis methods**

- Introduce a low-dimensional shape parametrization (**geometrical reduction**)
- Bring geometry variations back to the equation coefficients
- Evaluate PDEs/output using reduced basis methods (**computational reduction**)

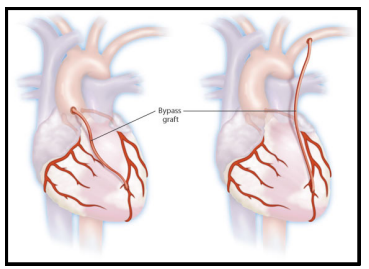

The curse of dimensionality in shape-related model reduction problems

- Computational complexity of **constructing the parametrized model** grows exponentially with the number of parameters, due to need to sample the parameter space
- Curse of dimensionality alleviated (but not eliminated) by better sampling strategies: sparse grids, latin hypercubes, adaptive sampling etc.
- Model reduction methods limited to small number of parameters (usually 5–10)
- Shapes are infinite-dimensional objects, large number of parameters needed to capture all possible variability if no a priori information available

How to represent shapes using parametrizations?

Shape families of diffeomorphic images of a reference domain

Ω $\Omega_o(\mu_1)$ $\Omega_o(\mu_2)$ $\Omega_o(\mu_3)$ $\Omega_o(\mu_4)$ $\Omega_o(\mu_5)$ $\Omega_o(\mu_6)$

- Reference domain $\Omega \subset \mathbb{R}^d$ with fixed computational mesh $\mathscr{T}_h$
- Define a parametric family of diffeomorphisms

$$T : \mathbb{R}^d \times \mathscr{D} \to \mathbb{R}^d \quad \text{s.t} \quad T(\cdot;\mu), T^{-1}(\cdot;\mu) \in W^{1,\infty}(\mathbb{R}^d;\mathbb{R}^d) \quad \text{for all } \mu \in \mathscr{D}$$

- Family of admissible shapes $\mathscr{O}_{\text{ad}}$ defined as

$$\mathscr{O}_{\text{ad}} := \{\Omega_o \subset \mathbb{R}^d : \Omega_o(\mu) = T(\Omega;\mu) \quad \text{for some } \mu \in \mathscr{D}\}$$

- Transformation of the PDE back to the reference domain by a change of coordinates

$$\int_{\Omega_o(\mu)} \nabla y_o \cdot \nabla w_o \, dx_o \quad \longmapsto \quad \int_\Omega \left[\nabla_x T(x,\mu)^{-T} \nabla_x T(x,\mu)^{-1}\right] \nabla y \cdot \nabla w \, |\det(\nabla_x T)| \, dx$$

  etc. for all the various bilinear forms in the weak form of the PDE

Limitation: All shapes Ω_o are diffeomorphic to each other $\Rightarrow$ topological properties fixed a priori.

Option #1: Piecewise affine transformations based on subdomain division

Construction:

- Divide into nonoverlapping subdomains $\overline{\Omega}_o = \bigcup_{k=1}^{K} \overline{\Omega}_o^k$
- Locally affine mappings on each subdomain

$$\overline{\Omega} o^k(\mu) = T^{\text{aff},k}(\overline{\Omega}^k;\mu), \quad s.t.$$

$$T_i^{\text{aff},k}(x;\mu) = C_i^{\text{aff},k}(\mu) + \sum_{j=1}^{d} G_{ij}^{\text{aff},k}(\mu) x_j, \quad 1 \le i \le d$$

- Global continuity condition

$$T^{\text{aff},k} = T^{\text{aff},k'} \text{ for all } x \in \overline{\Omega}^k \cap \overline{\Omega}^{k'}, 1 \le k < k' \le K$$

- Automatic decomposition tools in `rbMIT` (R., Huynh, Nguyen et al)

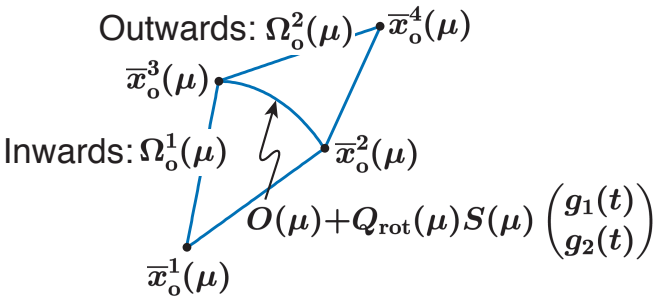

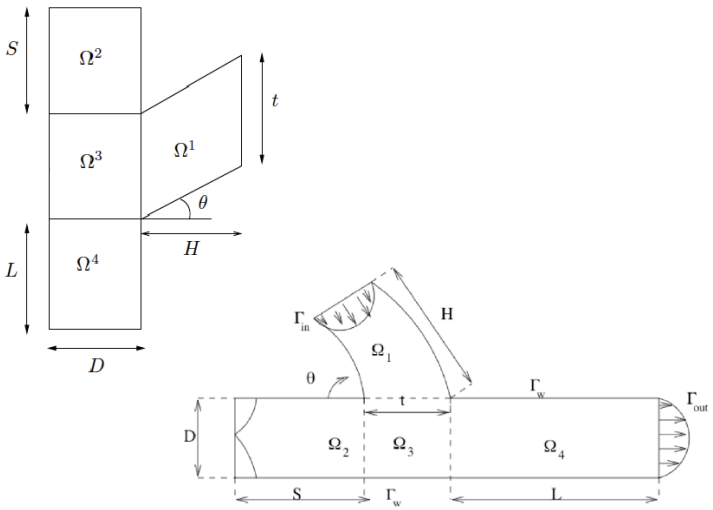

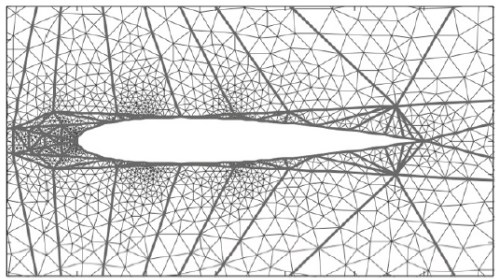

Option #2: Free-form deformation (with tensor Bernstein polynomials)

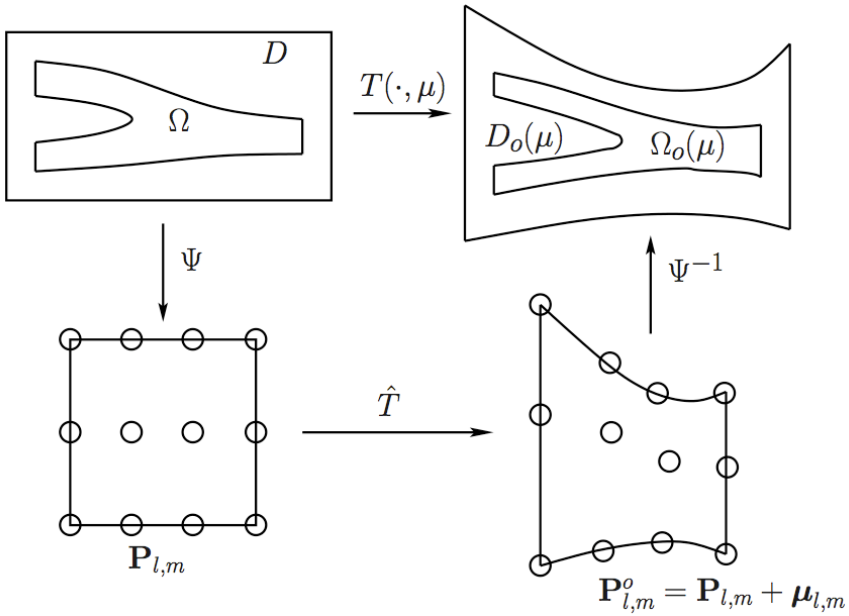

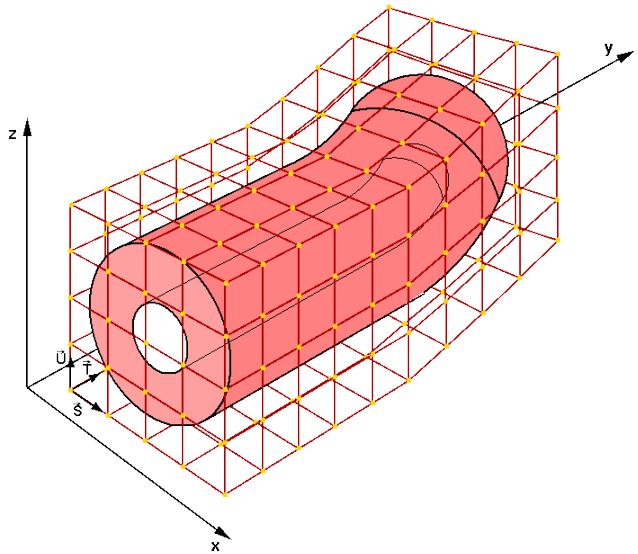

Construction:

- Parametric map: $T(\mathbf{x},\mu) = \sum_{l=0}^{L}\sum_{m=0}^{M} b_{l,m}^{L,M}(\Psi(\mathbf{x}))(\mathbf{P}_{l,m}+\mu_{l,m})$ where

$$b_{\ell,m}^{L,M}(s,t) = b_\ell^L(s)b_m^M(t) = \binom{L}{\ell}\binom{M}{m}(1-s)^{L-\ell}s^\ell(1-t)^{M-m}t^m$$

  are tensor products of Bernstein basis polynomials
- FFD mapping defined as $\Omega_o(\mu) = \Psi^{-1}\circ\hat{T}\circ\Psi(\Omega;\mu) =: T(\Omega;\mu)$
- Parameters $\mu_1,\ldots,\mu_P$ are displacements of selected control points

Option #2: Free-form deformation (with tensor Bernstein polynomials)

Example: shape optimization of a 3D bulb in a Stokes flow

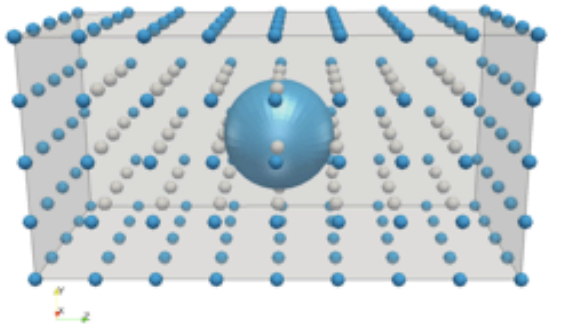

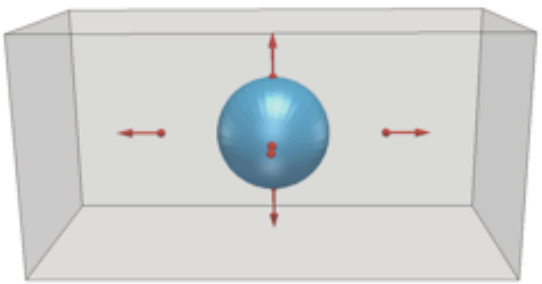

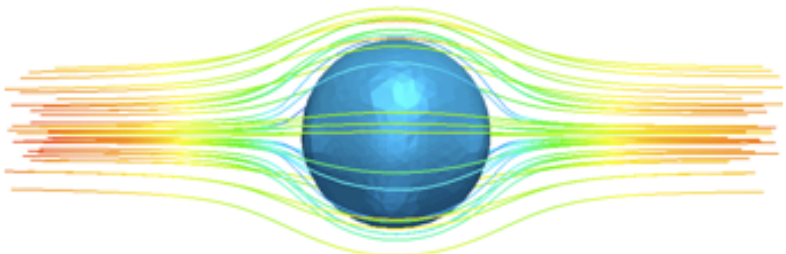

Shape optimization of a profile in a Stokes flow
(and comparison with the theoretical solution)
(constraint: fixed volume)

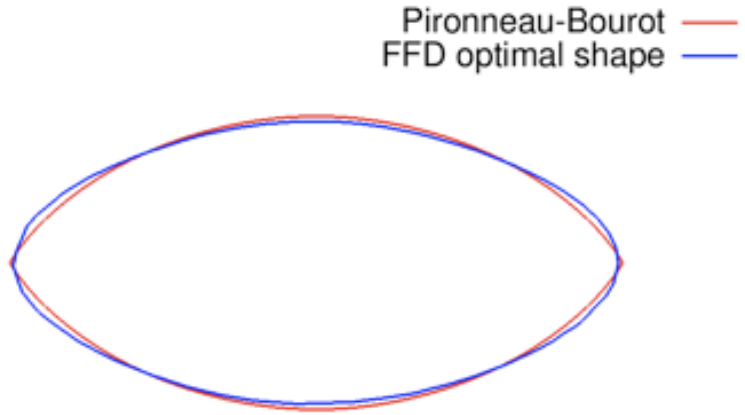

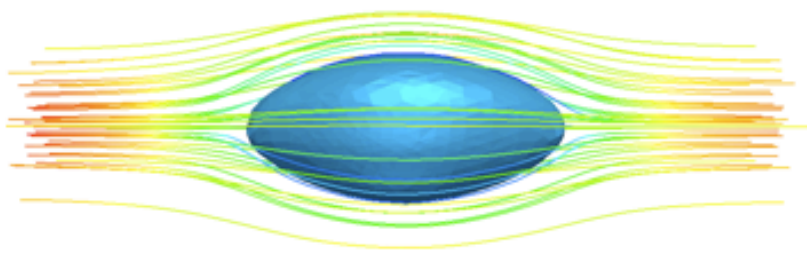

Images courtesy of F. Ballarin

Option #3: Radial basis functions

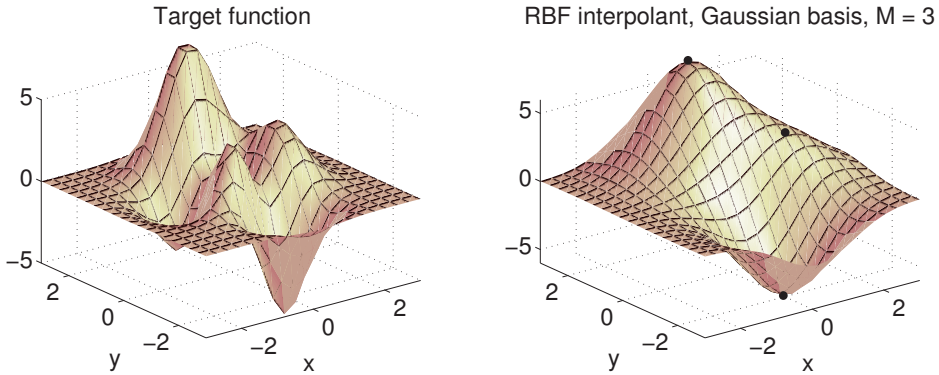

Construction:

- Set of scattered interpolation sites $\Xi := \{\mathbf{x}_m\}_{m=1}^{M} \subset \mathbb{R}^2$, not collinear.
- Shape function* $\varphi : \mathbb{R}_0^+ \to \mathbb{R}$ satisfying certain positivity constraints
- Deformation map defined under the form:

$$T(\mathbf{x}, \mu) = \mathbf{x} + \sum_{m=1}^{M} \mathbf{w}_m(\mu)\ \varphi(\|\mathbf{x} - \mathbf{x}_m\|)$$

where $\mathbf{w}_m(\mu)$ are obtained by solving the interpolation system

$$\begin{bmatrix} \varphi(\mathbf{x}_1 - \mathbf{x}_1) & \dots & \varphi(\mathbf{x}_1 - \mathbf{x}_M) \\ \vdots & \ddots & \vdots \\ \varphi(\mathbf{x}_M - \mathbf{x}_1) & \dots & \varphi(\mathbf{x}_M - \mathbf{x}_M) \end{bmatrix} \begin{bmatrix} \mathbf{w}_1^T(\mu) \\ \vdots \\ \mathbf{w}_M^T(\mu) \end{bmatrix} = \begin{bmatrix} \mu_1^T \\ \vdots \\ \mu_M^T \end{bmatrix},$$

i.e. parameters μ_m are the point values of an (**arbitrary**) displacement field at Ξ

*Possible choices: $\exp(-\alpha r^2)$ (Gaussian), $(r^2 + \alpha^2)^{1/2}$ (multiquadric), $\alpha |r|^3$ (cubic), etc.

Option #4: Transfinite interpolation -based maps

Ingredients:

- For each $\Gamma_i \subset \partial\Omega$, $i = 1, \ldots, n$, a weight function $\varphi_i : \Omega \to [0,1]$ and a projection function $\pi_i : \Omega \to [0,1]$, obtained as solution of a suitable Laplace problem on Ω
- For each edge $\Gamma_{oi} \subset \partial\Omega_o(\mu)$, a parametrized edge function $\psi_i(\cdot, \mu) : [0,1] \to \Gamma_{oi}$

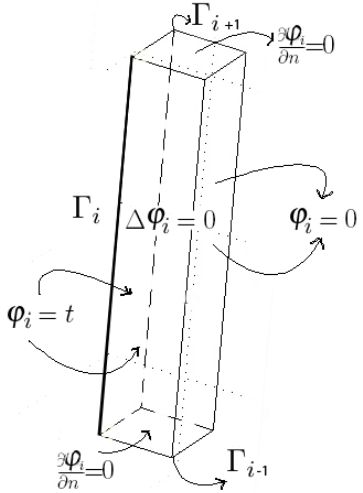

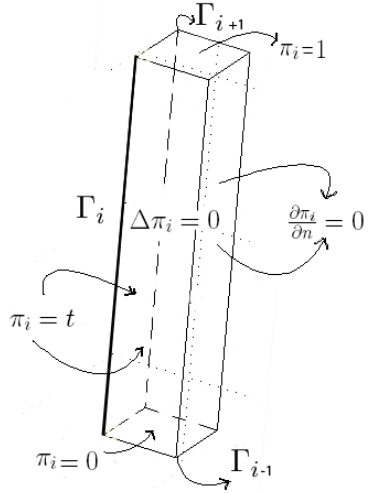

Construction:

$$T(\mathbf{x}, \mu) = \sum_{i=1}^{n} [\varphi_i(\mathbf{x})\psi_i(\pi_i(\mathbf{x}), \mu) - \varphi_i(\mathbf{x})\varphi_{i+1}(\mathbf{x})\psi_i(1, \mu)]$$

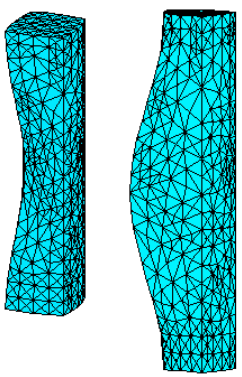

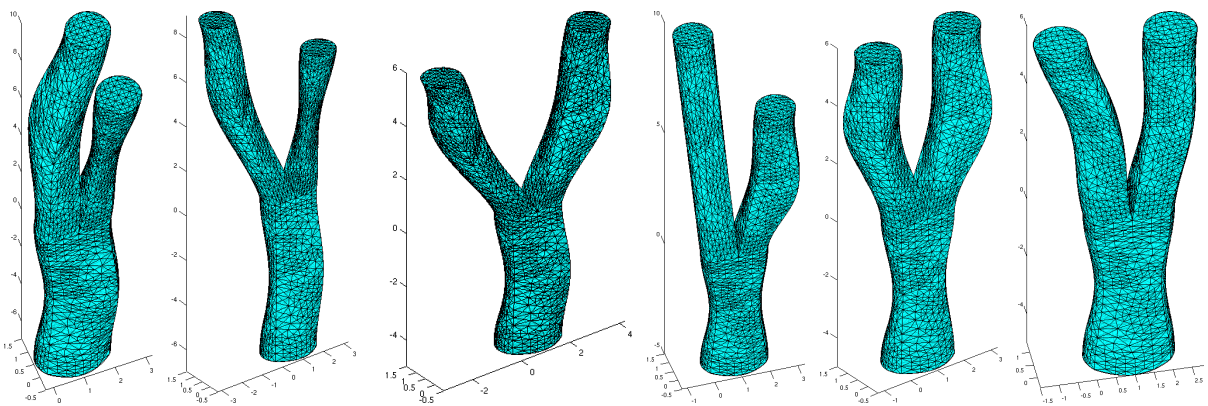

Images courtesy of L. Iapichino

Comparison of shape parametrization methods in model reduction

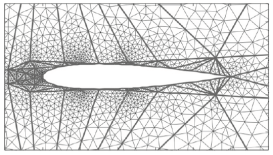

Piecewise affine

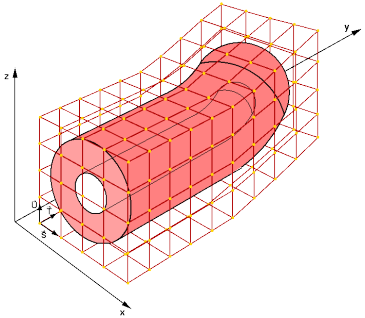

FFD

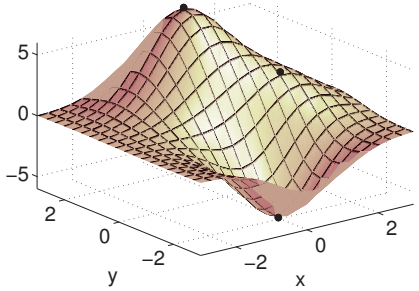

RBF

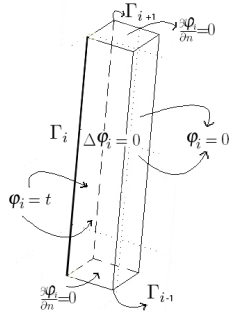

Transfinite maps

Parametrization method	**Pros**	**Cons**
Piecewise affine (Rozza/Veroy 2007, Rozza et al 2008)	+ Affine parametrization + Automatic in `rbMIT`	– Mesh dependent – Regularity only C^0 – Tedious to do by hand
FFD (Lassila/R. 2010, Manzoni/Quarteroni/R. 2011)	+ Mesh independent + Efficient implementations	– Tensor-product grid – Not interpolatory – Poor for rigid deforms
RBF (Manzoni/Quarteroni/R. 2012)	+ Mesh independent + Scattered control points + Interpolatory	– Choice of support size – Expensive evaluation
Transfinite maps (Løvgren/Maday/Rønquist 2006, Iapichino/Quarteroni/R. 2012)	+ Edge-based deformation	– Solving PDEs required – "Simple" geometries

Computational Reduction

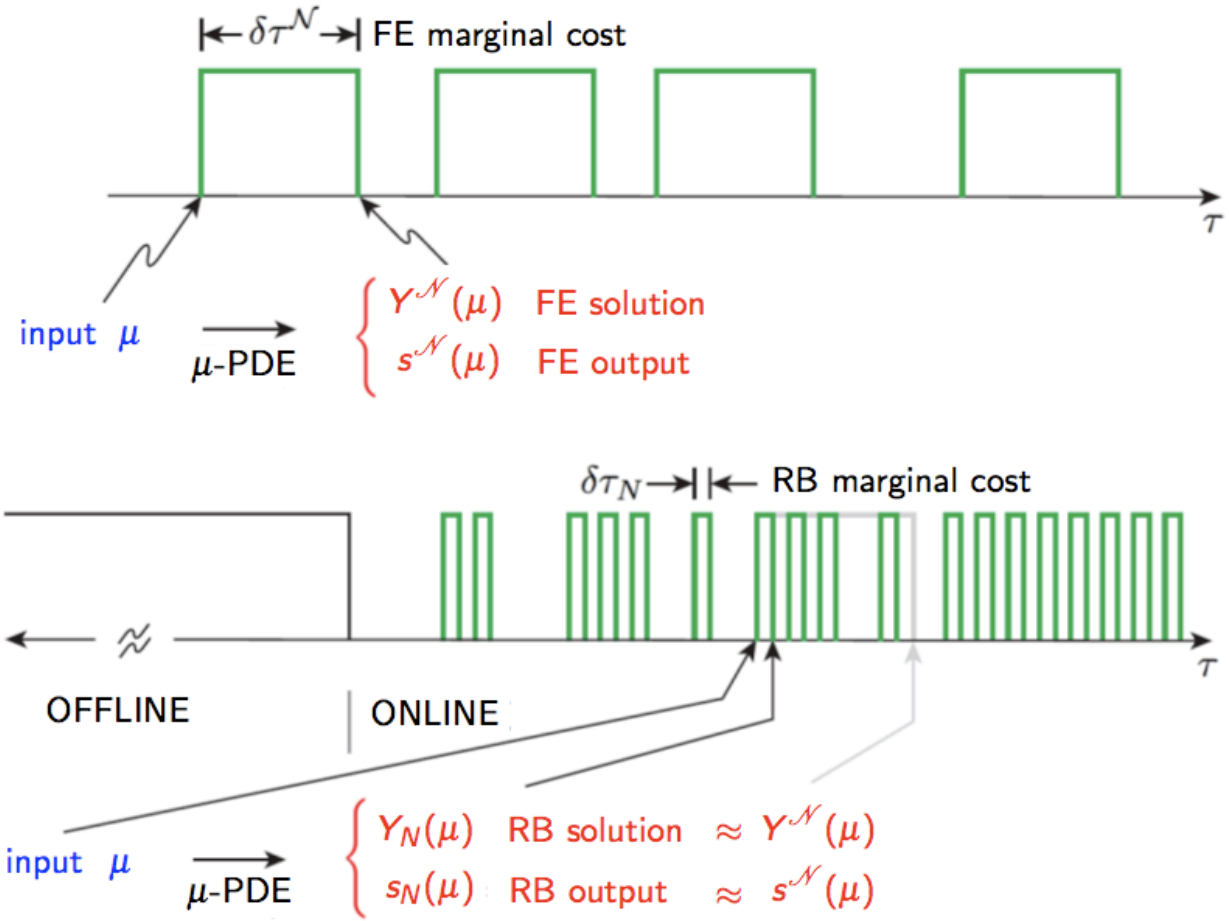

Acknowledgement: Anthony T. Patera (MIT) - `augustine.mit.edu`

Flow around parametrized airfoils

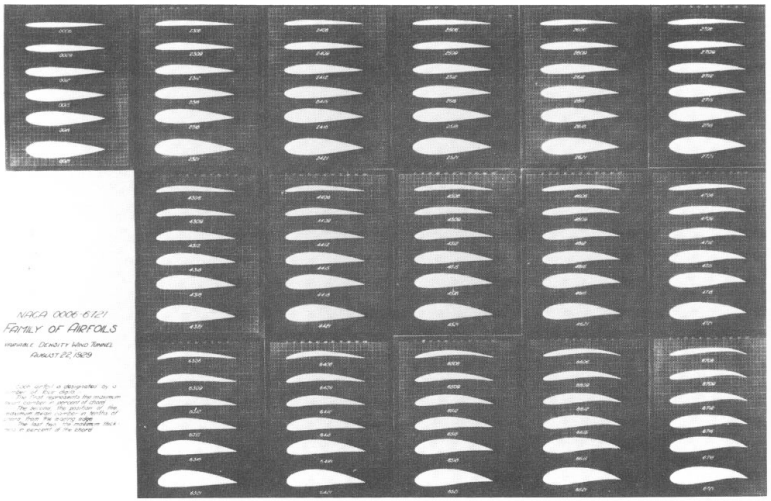

- Flow simulation around different airfoils within a NACA family
- evaluation of the airfoil performance (pressure coefficient)

Flow around parametrized airfoils

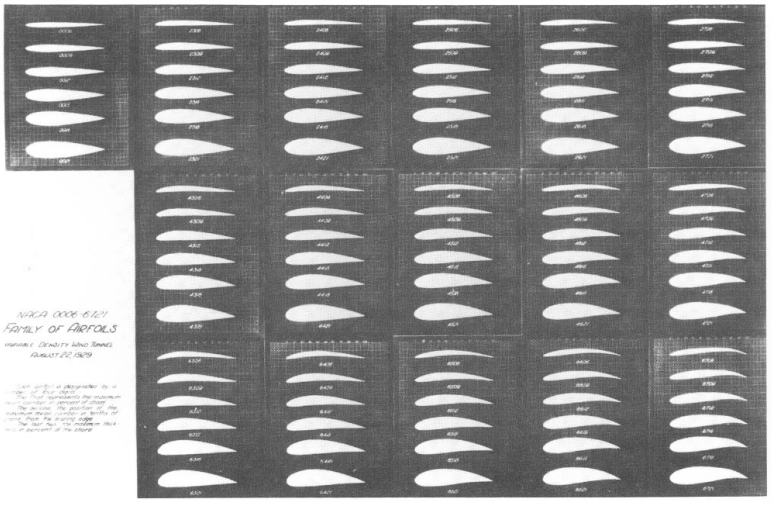

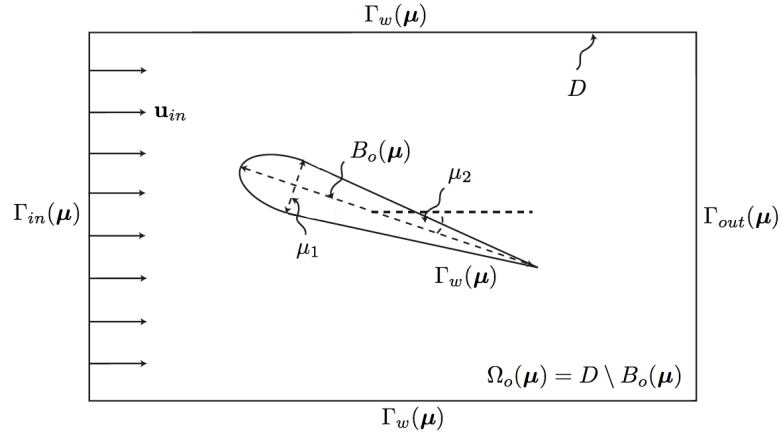

- Flow simulation around different airfoils within a NACA family
- evaluation of the airfoil performance (pressure coefficient)

Affine mappings based on domain decomposition and boundary parametrization

$$\mathbf{x}_o = \begin{pmatrix} 1 \\ 0 \end{pmatrix} + \begin{pmatrix} \cos\mu_2 & -\sin\mu_2 \\ \sin\mu_2 & \cos\mu_2 \end{pmatrix} \begin{pmatrix} -1 & 0 \\ 0 & \pm\mu_1/20 \end{pmatrix} \begin{pmatrix} 1-t^2 \\ \varphi(t) \end{pmatrix}, \quad t \in [0, \sqrt{0.3}]$$

$$\mathbf{x}_o = \begin{pmatrix} 0 \\ 0 \end{pmatrix} + \begin{pmatrix} \cos\mu_2 & -\sin\mu_2 \\ \sin\mu_2 & \cos\mu_2 \end{pmatrix} \begin{pmatrix} 1 & 0 \\ 0 & \pm\mu_1/20 \end{pmatrix} \begin{pmatrix} t^2 \\ \varphi(t) \end{pmatrix}, \quad t \in [\sqrt{0.3}, 1],$$

$$\varphi(t) = 0.2969t - 0.1260t^2 - 0.3520t^4 + 0.2832t^6 - 0.1021t^8$$

thickness $\mu_1 \in [4, 24]$, angle of attack $\mu_2 \in [0, \pi/4]$

Flow around parametrized airfoils

Laplace equation(velocity potential):

$$
\begin{aligned}
-\Delta\phi &= 0 && \text{in } \Omega_o(\mu)\\
\frac{\partial\phi}{\partial\mathbf{n}} &= 0 && \text{on } \Gamma_{\text{w}}(\mu)\\
\frac{\partial\phi}{\partial\mathbf{n}} &= \phi_{\text{in}} && \text{on } \Gamma_{\text{in}}(\mu)\\
\phi &= \phi_{\text{ref}} && \text{on } \Gamma_{\text{out}}(\mu),
\end{aligned}
$$

Pressure and velocity:

$$\mathbf{v} = \nabla\phi$$

$$p + \frac{1}{2}\rho|u|^2 = p_{\text{in}} + \frac{1}{2}\rho|v_{\text{in}}|^2, \quad \text{in } \Omega_o(\mu),$$

Pressure coefficient

$$c_p(p) = \frac{p - p_{\text{in}}}{\frac{1}{2}\rho|u_{\text{in}}|^2} = 1 - \left(\frac{|u|^2}{|u_{\text{in}}|^2}\right),$$

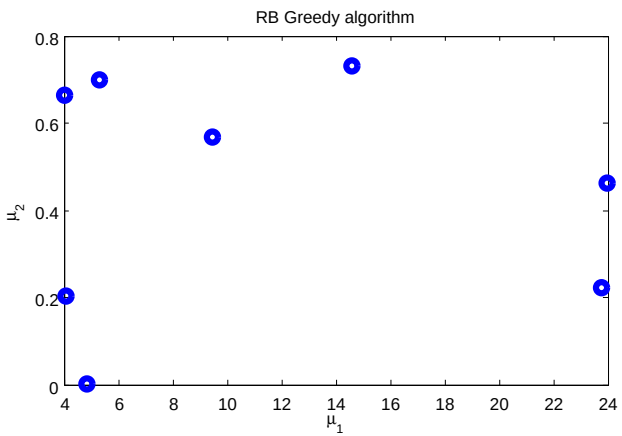

Greedy sampling (parameter space)

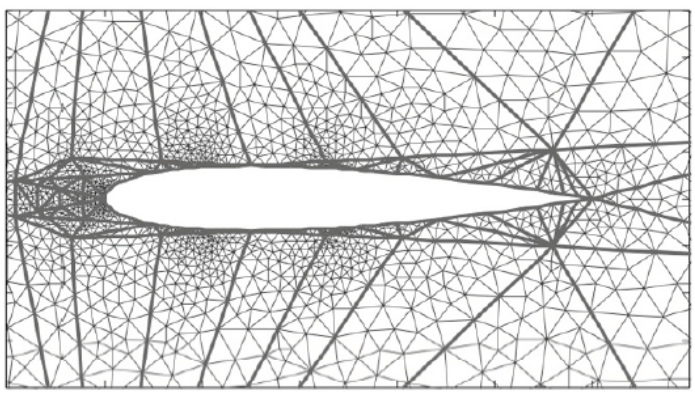

Automatic affine maps + domain decomposition

Flow around parametrized airfoils

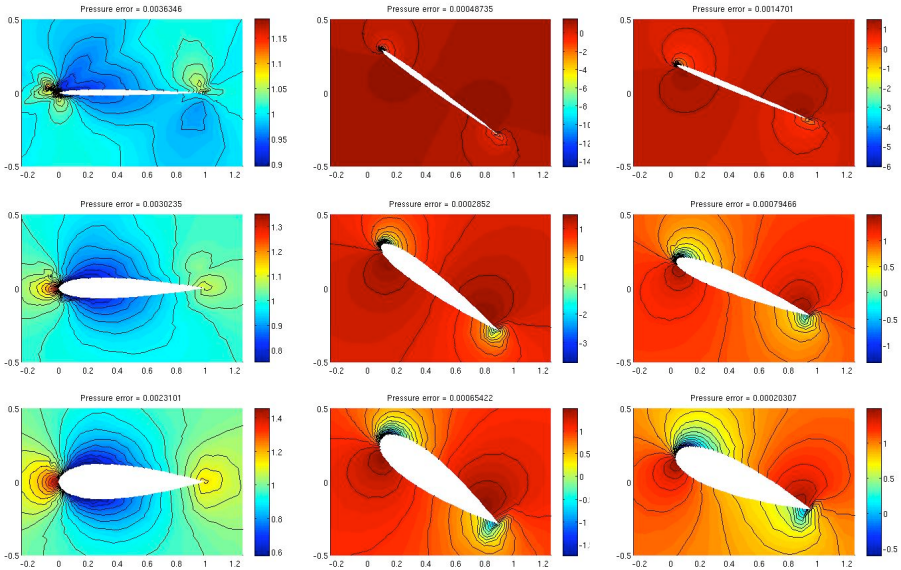

pressure fields

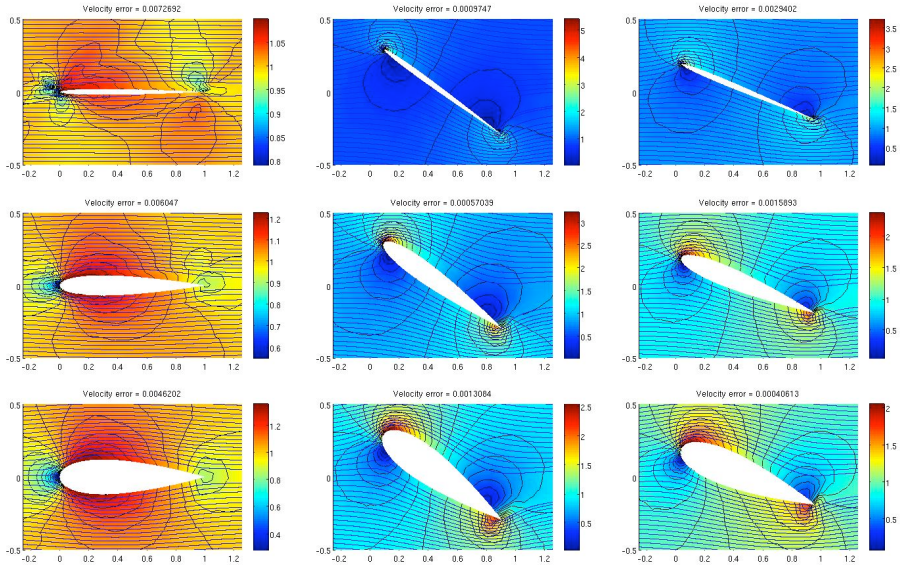

velocity fields

Number of FE dof $\mathcal{N}$	$\approx 3,500$
Number of RB basis functions N	8
Automatic affine domain decomposition	$t_{FE}^{offline} = 8h$
Greedy algorithm + RB structures/space	$t_{RB}^{offline} = 4h$
Computational speedup	$t_{RB}^{online} / t_{FE}^{online} = 250^3$

[3] Computations carried out on a single processor of a 2GHz Dual Core AMD Opteron(tm), processors 2214 HE and 16 GB of RAM

Flow around parametrized airfoils

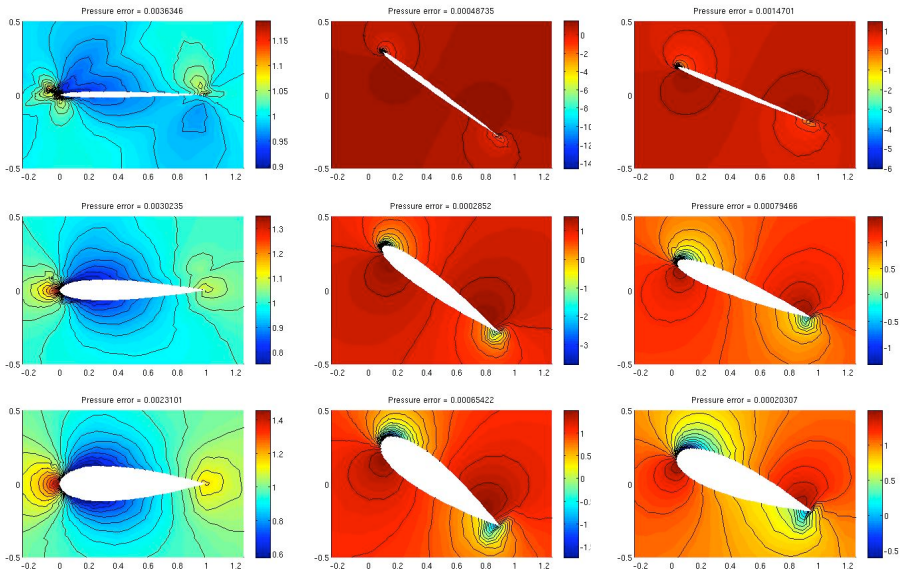

pressure fields

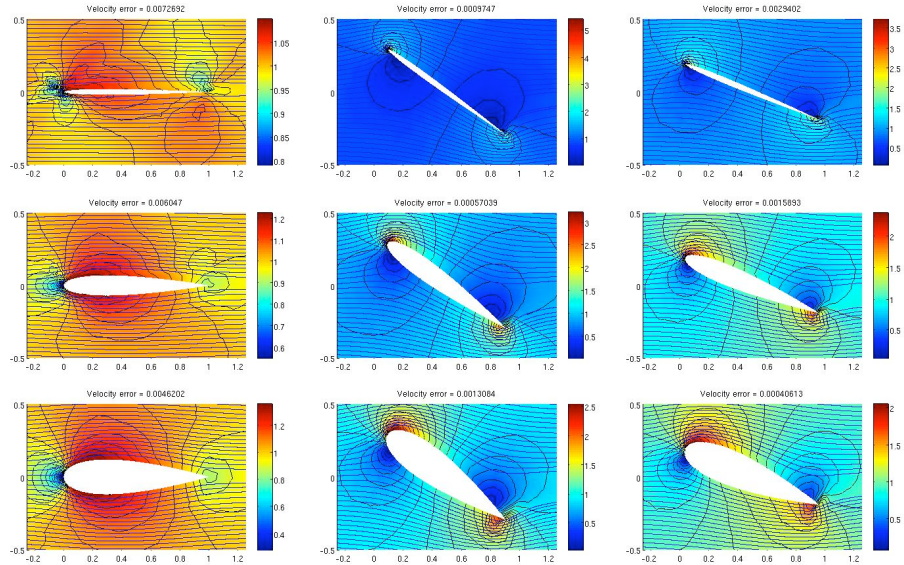

velocity fields

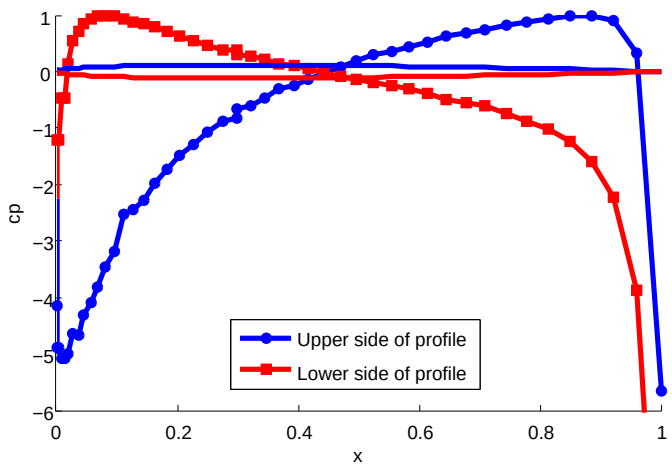

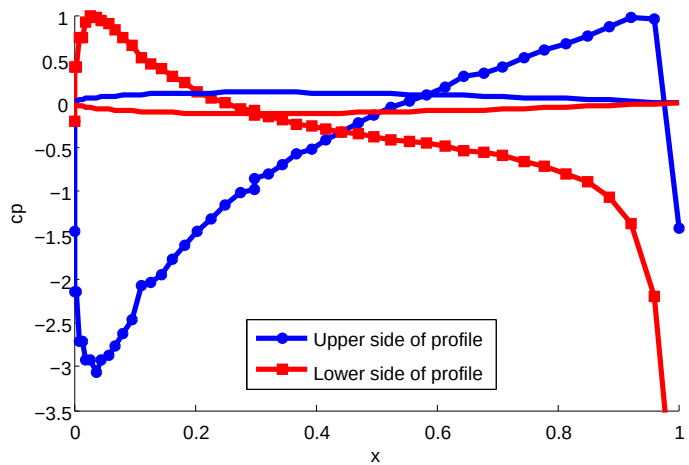

Pressure coefficients for two different NACA airfoils

[3] Computations carried out on a single processor of a 2GHz Dual Core AMD Opteron(tm), processors 2214 HE and 16 GB of RAM

Flow around parametrized airfoils

Other possible options

FFD

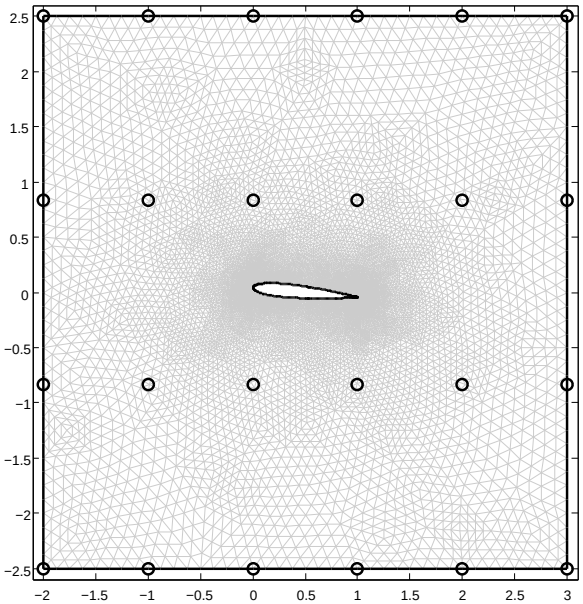

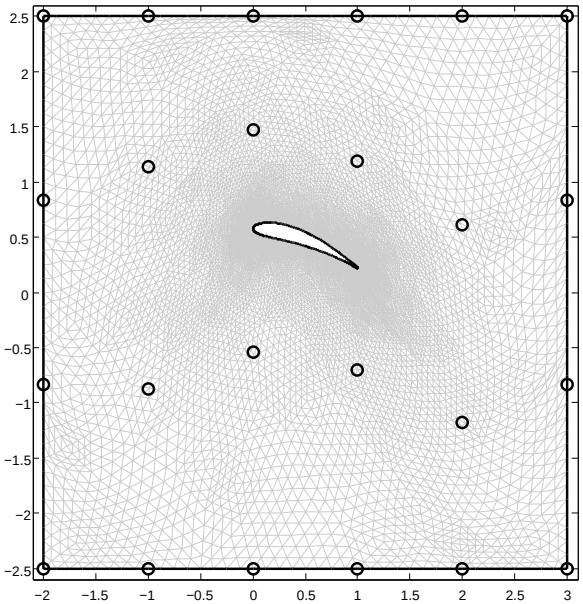

RBF

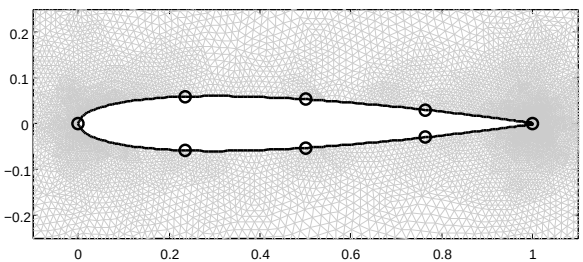

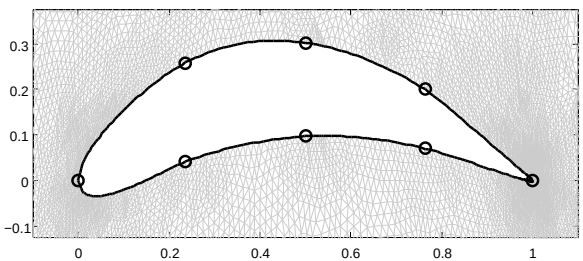

Flow across parametrized carotid bifurcations

Vessels geometry strongly influences haemodynamics behaviour

- Study the influence of the vessel shape on blood flow
- Real-time evaluation of flow indexes related with geometry variation that assess/measure arteries occlusion risk (e.g. vorticity, viscous energy dissipation) [Manzoni, Quarteroni, R. 11]

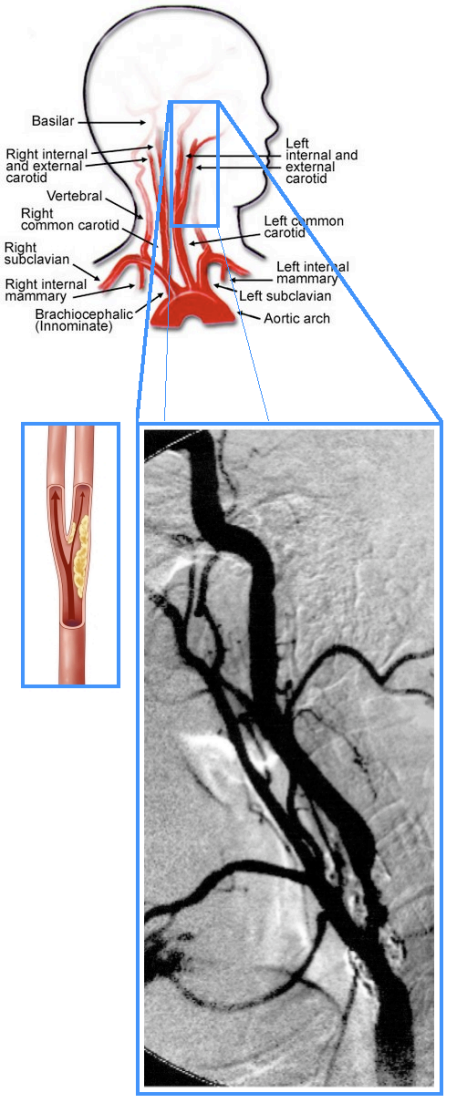

Output evaluation problem:

$$\text{evaluate} \quad J_o(\Omega_o;\mathbf{v}) = \int_{\Omega_o} |\nabla \mathbf{v}|^2 d\Omega_o \quad \text{s.t.}$$

$$\begin{cases} -\nu\Delta\mathbf{v} + (\mathbf{v}\cdot\nabla)\mathbf{v} + \nabla p = \mathbf{f} & \text{in } \Omega_o \\ \nabla\cdot\mathbf{v} = 0 & \text{in } \Omega_o \\ \mathbf{v} = \mathbf{v}_g & \text{on } \Gamma_w^o := \partial\Omega_o \setminus \Gamma_{out}^o, \\ -p\cdot\mathbf{n} + \nu\dfrac{\partial\mathbf{v}}{\partial\mathbf{n}} = \mathbf{0} & \text{on } \Gamma_{out}^o \end{cases}$$

A case of interest: carotid artery bifurcation (e.g. in presence of stenosis)

- **Shape reconstruction through parameter identification**
- **Shape sensitivity analysis**

Flow across parametrized carotid bifurcations

Family of healthy carotid bifurcations (intra-patients variability)

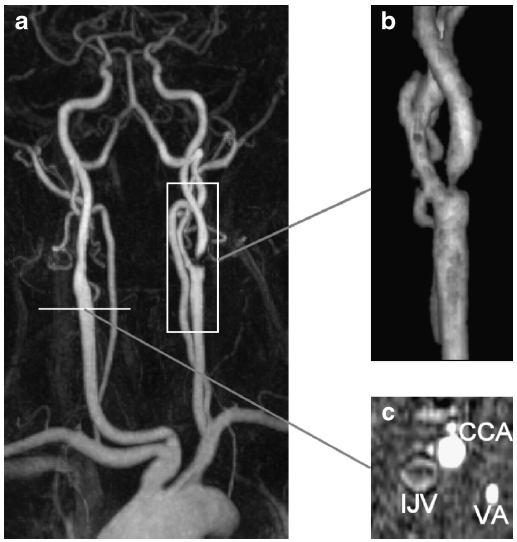

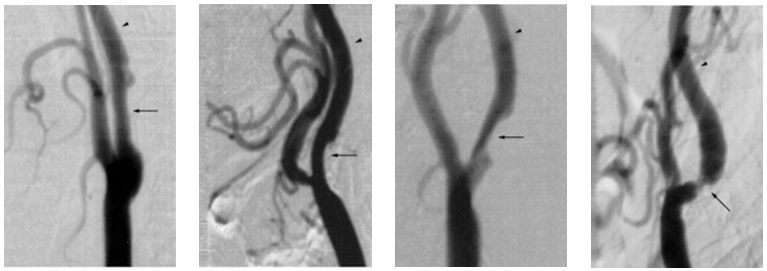

Family of stenosed carotid bifurcations (stenosis growth as shape change)

Flow across parametrized carotid bifurcations

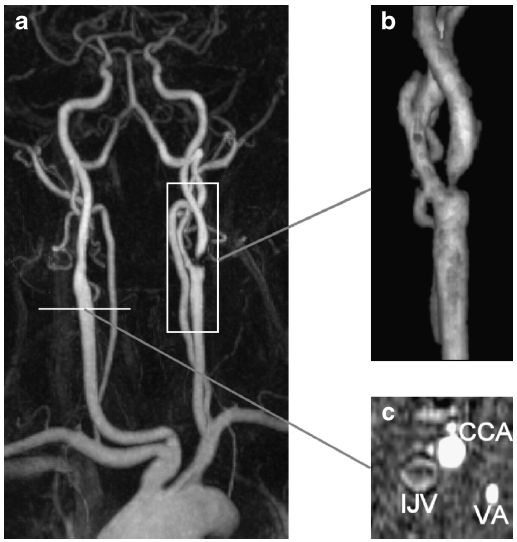

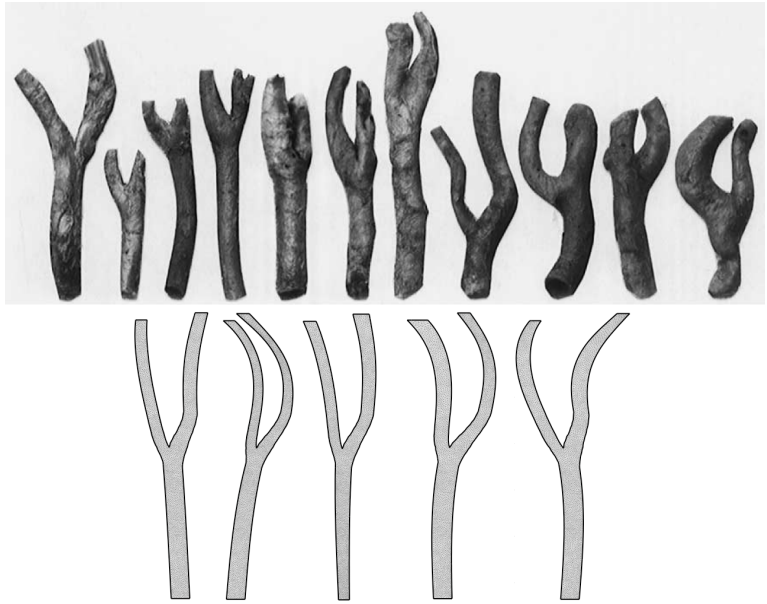

Family of healthy carotid bifurcations (intra-patients variability)

Global deformations (RBF with $\varphi(r) = r^3$)

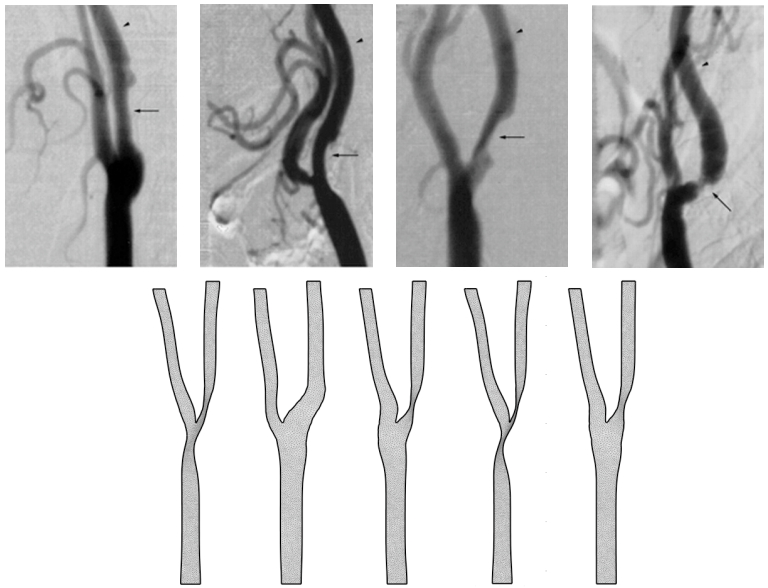

Family of stenosed carotid bifurcations (stenosis growth as shape change)

Local deformations (RBF with $\varphi = \exp(-r^2)$)

Flow across parametrized carotid bifurcations

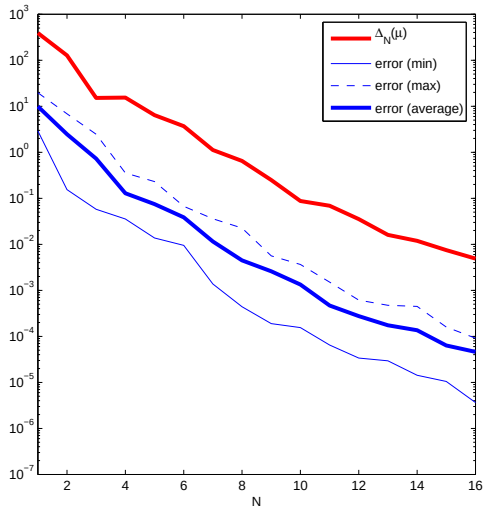

Number of FE dof $\mathcal{N}_{\mathbf{v}} + \mathcal{N}_p$	24046
Number of RB functions N	16
Number of design variables P	7

Nonlinear system dimension reduction	500:1
FE evaluation t_{FE} (s)	217.76
RB evaluation t_{RB}^{online} (s)	2.31

• Error estimation and • true error RB vs. FE approximation

Shape reconstruction

t = 5.35s

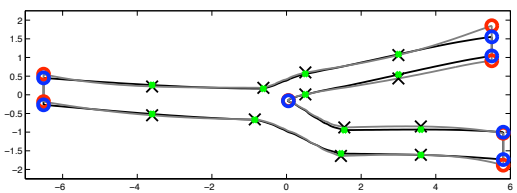

RB flow simulation

t = 2.31s

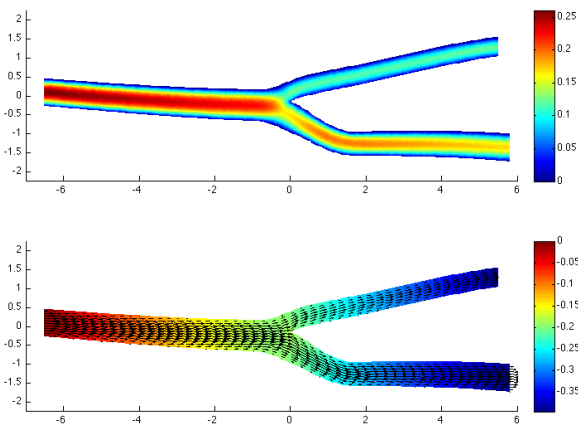

Output evaluation

t = 1.54s

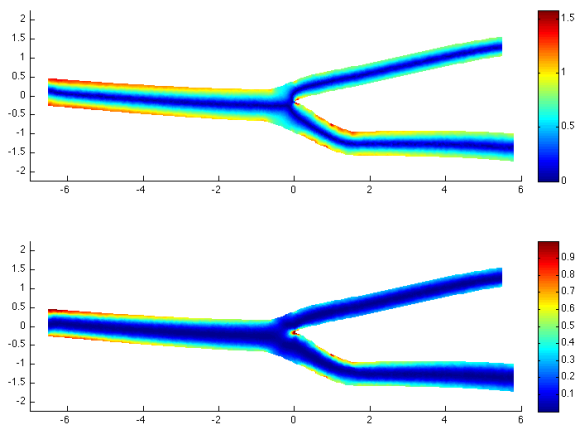

Computational times are obtained as an average over 50 shape reconstructions/RB Online evaluations

Flow across parametrized carotid bifurcations

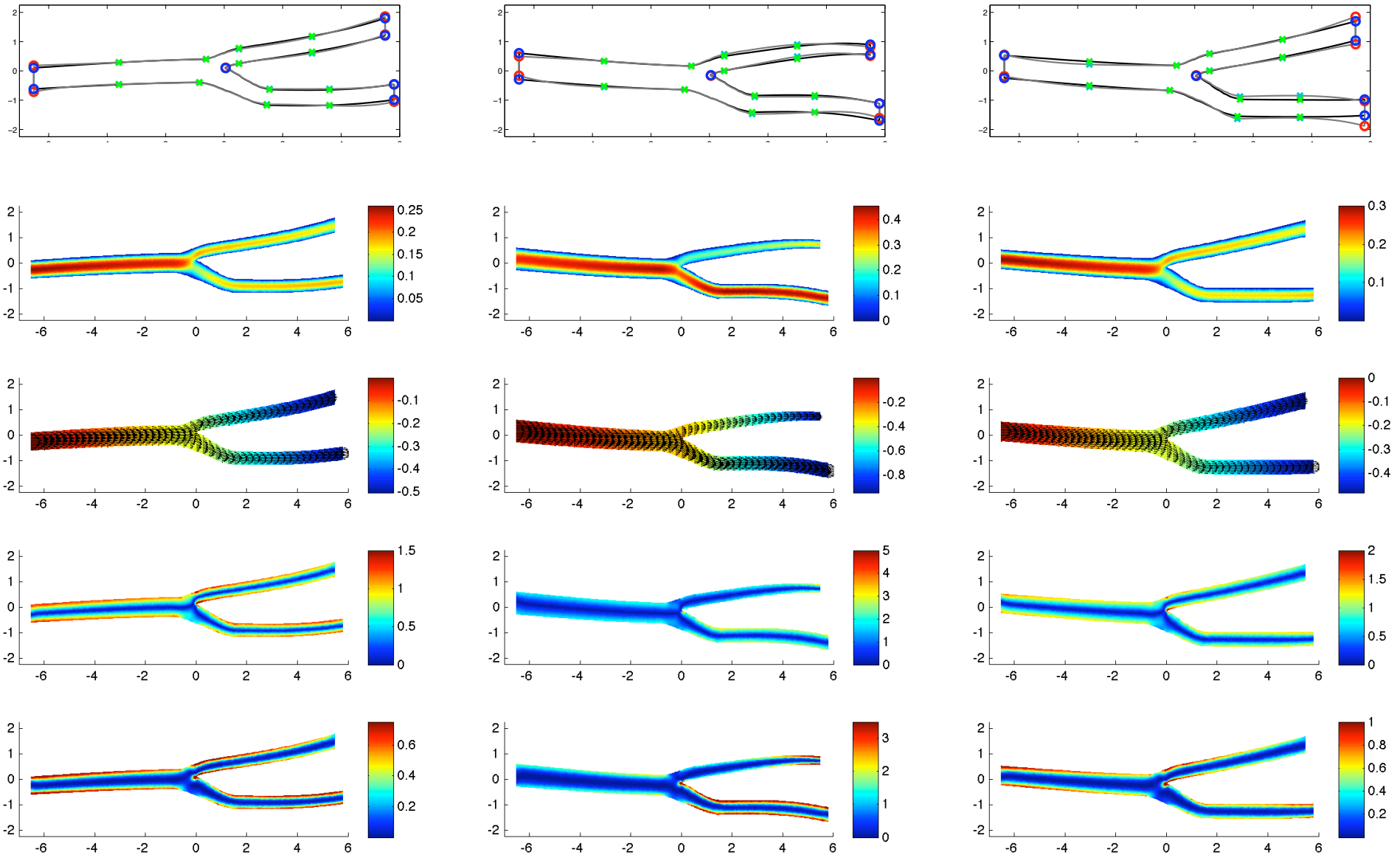

Reconstructed and target shapes, velocity and pressure fields, vorticity and viscous stresses

Flow across parametrized carotid bifurcations

Flow sensitivity analysis wrt large local shape deformations

Shape Parametrization: RBF, Gaussian kernel ($\phi(r) = exp(-r^2)$), $P = 4$ input parameter (displacements of • control points)

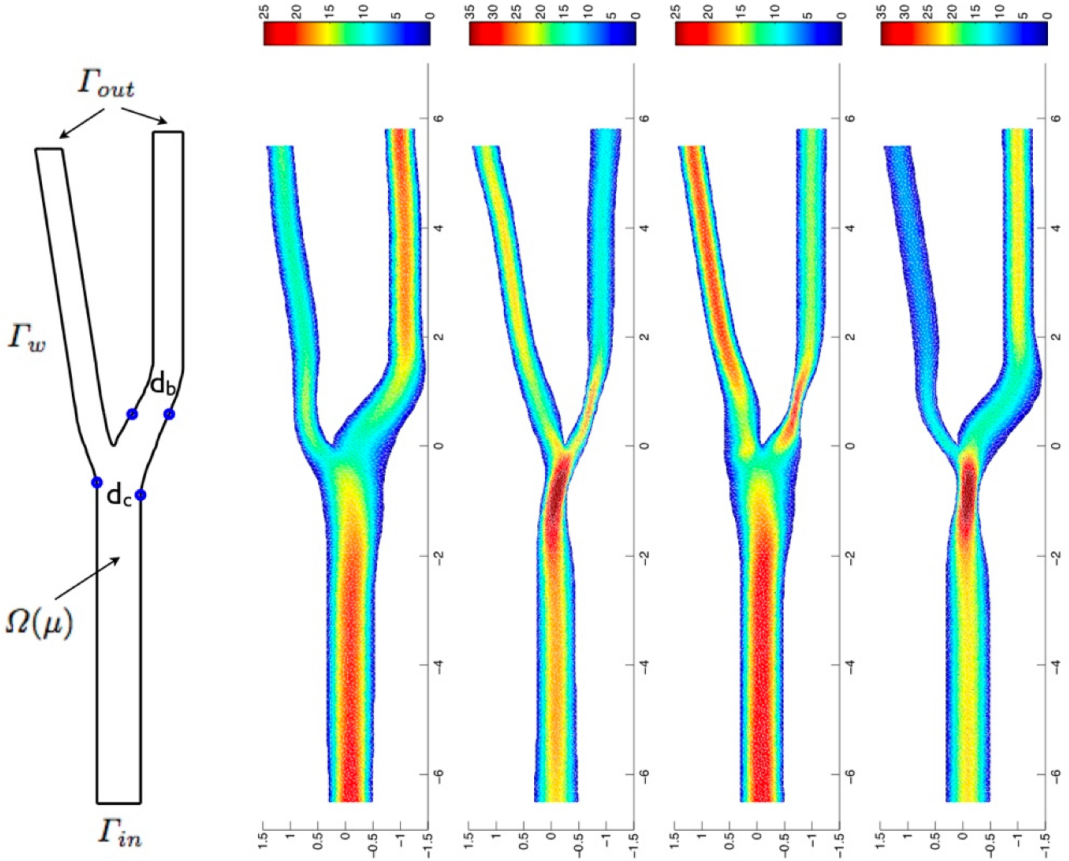

Velocity profiles $[cm/s]$ in four different carotid bifurcations parametrized wrt the diameters $d_c = d_c(\mu_1, \mu_2)$ of the CCA at the bifurcation and $d_b = d_b(\mu_3, \mu_4)$ of the mid-sinus level of the ICA.

Affine components Q	62
FE space dim. $\mathcal{N}_{\mathbf{v}} + \mathcal{N}_p$	$\approx 26,000$
RB space dim. N_{max}	15

FE evaluation t_{FE}^{online} (s)	1,125
RB evaluation t_{RB}^{online} (s)	2.47
Computational speedup	456

Flow across parametrized carotid bifurcations

Flow sensitivity analysis wrt large local shape deformations

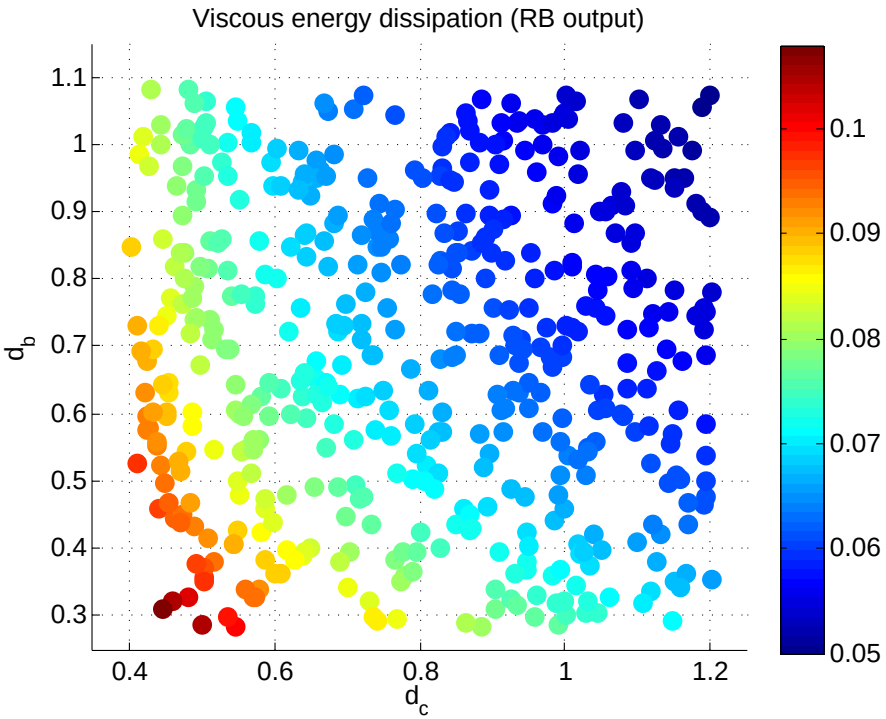

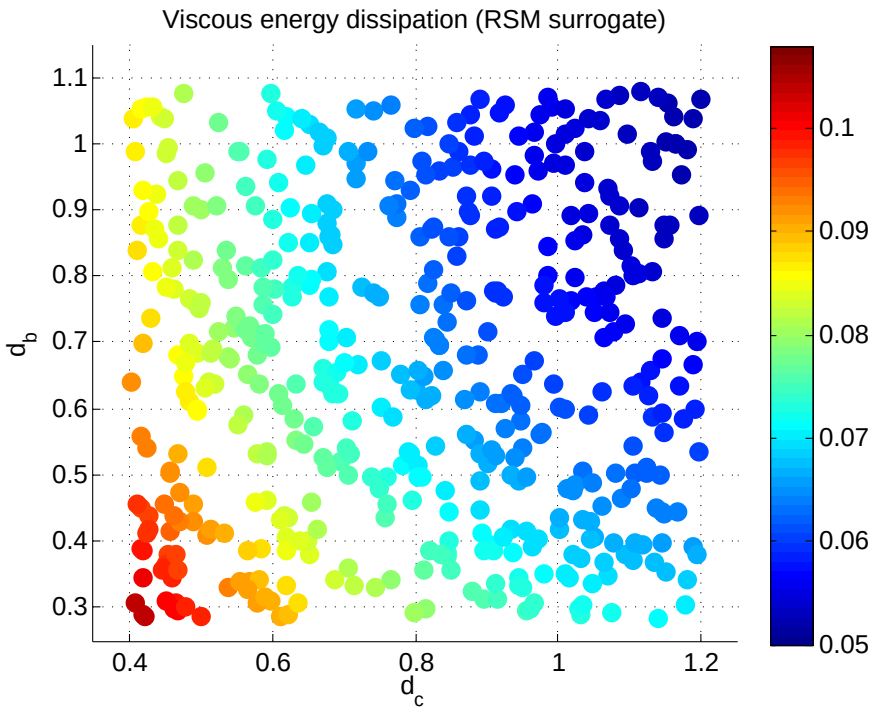

Left: Computed values of the viscous energy dissipation $J_N(\mu)$ for $n_{\text{test}} = 500$ cases (RB approximation).

Right: Viscous energy dissipation $J_{RSM}(\mu)$ computed through a quadratic response surface

Flow Control and Optimal Design with Reduced Basis Methods

using Free-Form Deformation Techniques

ÉCOLE POLYTECHNIQUE
FÉDÉRALE DE LAUSANNE

Example 1: Potential Flow Optimization Problem

Airfoil inverse design problem

$$\min_{\mu\in\mathcal{D}} \quad \left(\int_0^1 |p(s,\mu)-p_{\text{target}}(s)|^2\,ds\right)^{1/2} + \lambda\,[\alpha(\mu)-5^\circ]^2,$$

$$\text{s.t.} \quad \int_{\Omega_o(\mu)} \nabla u\cdot\nabla v\,d\Omega_o = \int_{\Omega_o(\mu)} fv\,d\Omega_o \;\forall v\in H^1(\Omega_o(\mu))$$

$$u=0 \text{ on } \Gamma_{out}, \quad \frac{\partial u}{\partial n}=-1 \text{ on } \Gamma_{in}, \quad \frac{\partial u}{\partial n}=0 \text{ elsewhere}$$

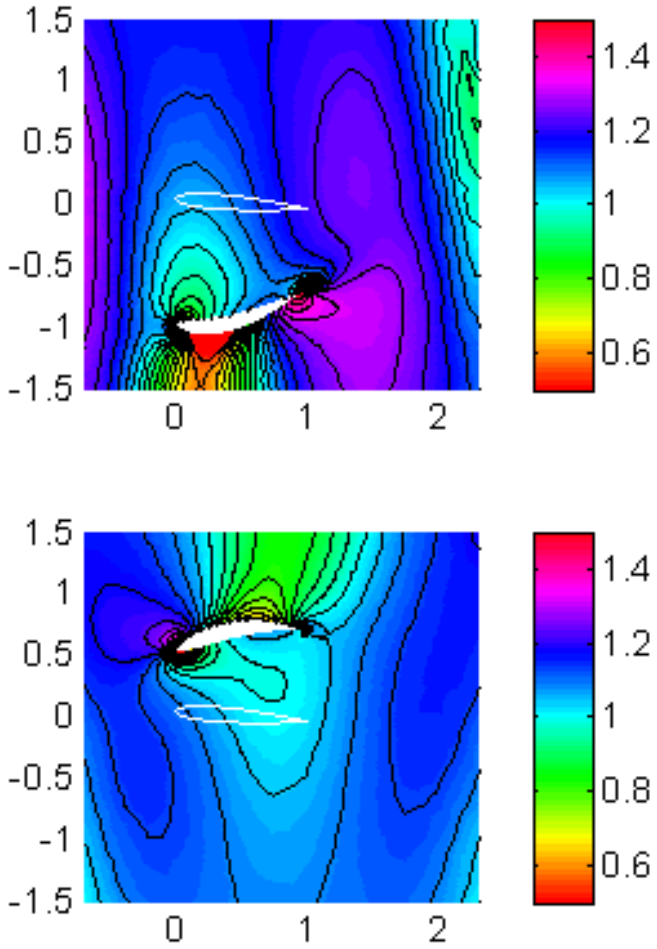

- Choose target airfoil (ex: NACA4412) and compute pressure distribution p_{target} on its surface using the Bernoulli equation ($p = p_0 - \frac{1}{2}|\nabla u|^2$)
- Objective: find small perturbation of reference airfoil NACA0012 s.t. pressure distribution on the airfoil surface is close to p_{target}
- Add penalty term to enforce the constraint on the angle of attack (AOA = 5°)

ÉCOLE POLYTECHNIQUE FÉDÉRALE DE LAUSANNE

Free-Form Deformations in Action

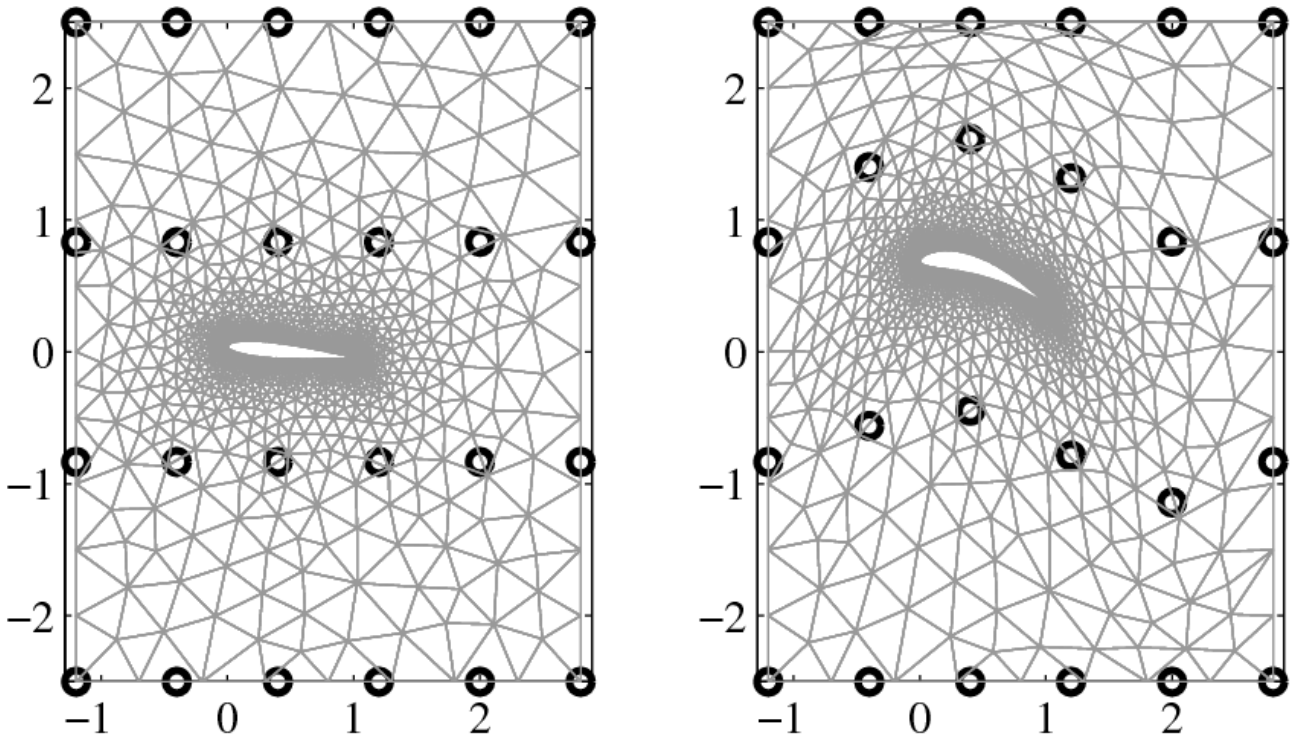

Figure: An example of the reference airfoil and a deformed configuration.

ÉCOLE POLYTECHNIQUE
FÉDÉRALE DE LAUSANNE

Example 1: Approximation Details

Pressure distributions and computational cost (online solution of the parametric PDE)

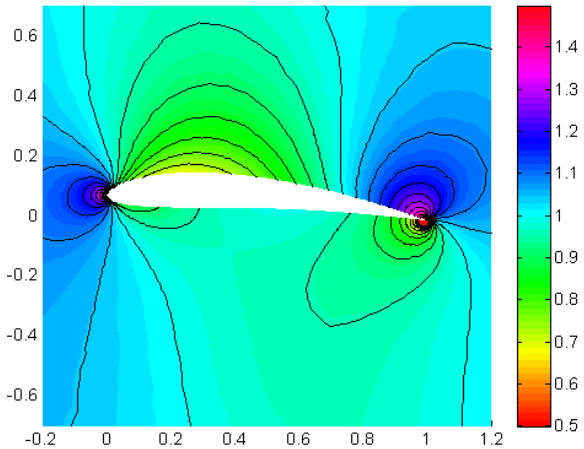

Inverse design

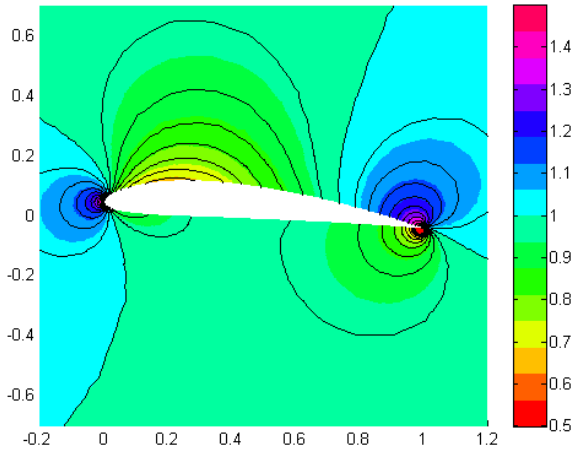

Target airfoil NACA4412

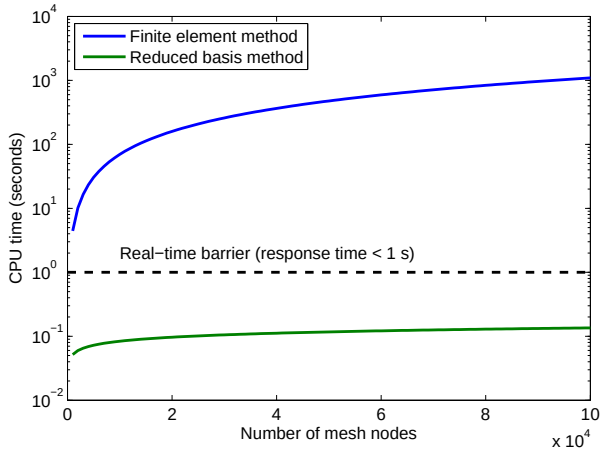

Computational costs

Number of mesh nodes $\mathcal{N}$	8043
Lattice of FFD control points $\boldsymbol{P}_{i,j}$	6×4
Number of shape parameters*	8
Number of reduced basis functions $N^{\dagger}$	52
Error tolerance for RB greedy ε_{tol}^{RB}	10^{-4}
Number of affine expansion terms Q_a	80
Error tolerance for EIM greedy ε_{tol}^{EIM}	2.5×10^{-3}

*Reduction of 50:1 in parametric complexity compared to explicit nodal deformation

†Reduction of 200:1 in linear system dimension

ÉCOLE POLYTECHNIQUE FÉDÉRALE DE LAUSANNE

Example 2: Optimal Design of Airfoils in Thermal Flows

Optimal heat exchange problem

$$\min_{\mu\in\mathscr{D}} \quad \left[\overline{u}_{target} - \frac{1}{|\Gamma_{out}|}\int_{\Gamma_{out}} u(\boldsymbol{x})\, d\Gamma\right]^2 + \lambda\left[\alpha(\mu)-\alpha_0\right]^2,$$

$$\text{s.t.} \quad \int_{\Omega_o(\mu)}\left(\varepsilon\nabla u\cdot\nabla v + v\vec{b}\cdot\nabla u\right) d\Omega_o = \int_{\Omega_o(\mu)} fv\, d\Omega_o$$

$$\frac{\partial u}{\partial n} = 0 \text{ on } \Gamma_{out},\ u = T_0 \text{ on } \Gamma_{in}\cup\Gamma_{free},$$

$$u = T_1 \text{ on } \Gamma_{surf},\quad u = T_2 \text{ on airfoil}$$

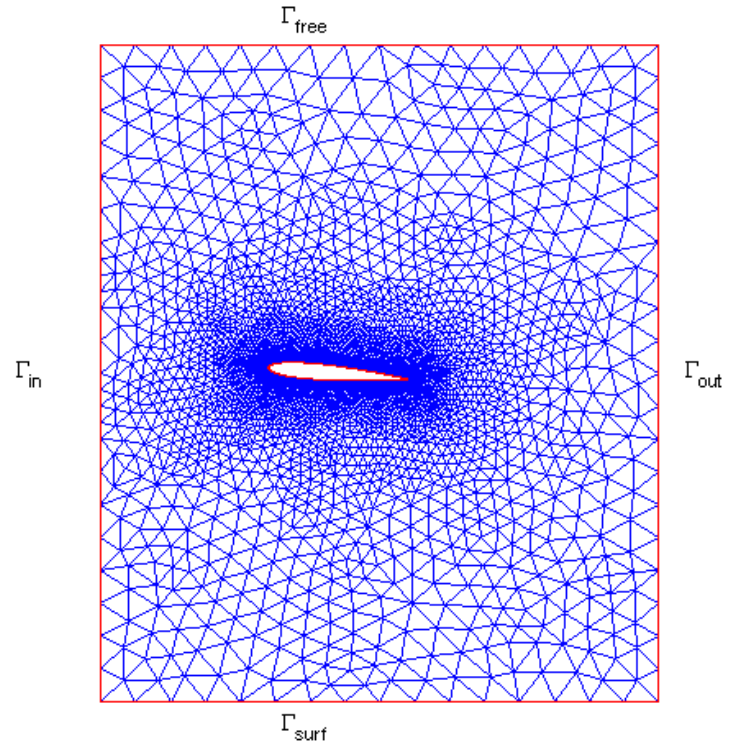

- Objective: find airfoil shape and vertical position s.t. average temperature over outflow equals $\overline{u}_{target}$ and angle of attack equals α_0
- Heat exchange of an airfoil in exterior flow with $\vec{b} = [1;0]$ and $\varepsilon = 0.2$ is considered
- Penalty term enforces the constraint on the angle of attack (AOA = α_0)

ÉCOLE POLYTECHNIQUE FÉDÉRALE DE LAUSANNE

Example 2: Approximation Details

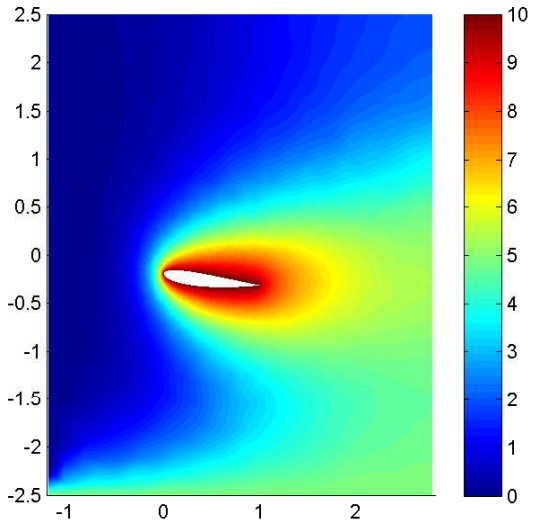

$\alpha_0 = 7^\circ$, $\overline{u}_{target} = 4.1$

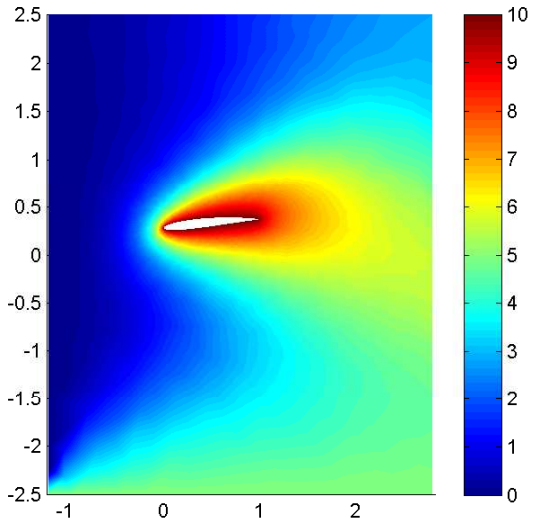

$\alpha_0 = -5^\circ$, $\overline{u}_{target} = 4.5$

Number of mesh nodes $\mathcal{N}$	15718
Lattice of FFD control points $\boldsymbol{P}_{i,j}$	6×6
Number of shape parameters*	8
Number of reduced basis functions $N^\dagger$	36
Error tolerance for RB greedy ε_{tol}^{RB}	10^{-5}
Number of affine expansion terms Q_a	108
Error tolerance for EIM greedy ε_{tol}^{EIM}	10^{-4}

*Reduction of 100:1 in parametric complexity compared to explicit nodal deformation

†Reduction of 436:1 in linear system dimension

ÉCOLE POLYTECHNIQUE FÉDÉRALE DE LAUSANNE

Example 3: Bypass Anastomosis Shape Optimization

Aorto-coronaric bypass shape design problem

$$\min_{\mu\in\mathcal{D}} \quad \frac{\gamma}{2}\int_{\Omega_O^C(\mu)} |\nabla\times\mathbf{u}(\mu)|^2\, d\Omega_o, \qquad \Omega_O^C(\mu)\subseteq\Omega_o(\mu)$$

$$\text{s.t.}\begin{cases} \nu\displaystyle\int_{\Omega_o(\mu)} \nabla\mathbf{u}\cdot\nabla\mathbf{w}d\Omega_o - \int_{\Omega_o(\mu)} p\nabla\cdot\mathbf{w}d\Omega_o = \int_{\Omega_o(\mu)} \mathbf{f}\cdot\mathbf{w}d\Omega_o & \forall\mathbf{w}\in(H^1_{0,\Gamma_D}(\Omega_o(\mu)))^2, \\ \displaystyle\int_{\Omega_o(\mu)} q\nabla\cdot\mathbf{u}d\Omega_o = 0 & \forall q\in L^2(\Omega_o(\mu)), \\ \mathbf{u}=\mathbf{g} \text{ on } \Gamma_D, \qquad \nu\frac{\partial\mathbf{u}}{\partial\mathbf{n}} - p\mathbf{n} = \mathbf{0} \text{ on } \Gamma_N \end{cases}$$

- Focal intimal thickening affects the long-term efficacy of coronary bypass procedures; geometry changes affect vorticity, shear stress and shear stress gradient
- Objective: find an optimal aorto-coronaric bypass anastomosis shape s.t. vorticity is minimized in a given subregion $\Omega_O^C(\mu)$ of the downfield branch
- Requirement: allow general deformations using a small parameters set

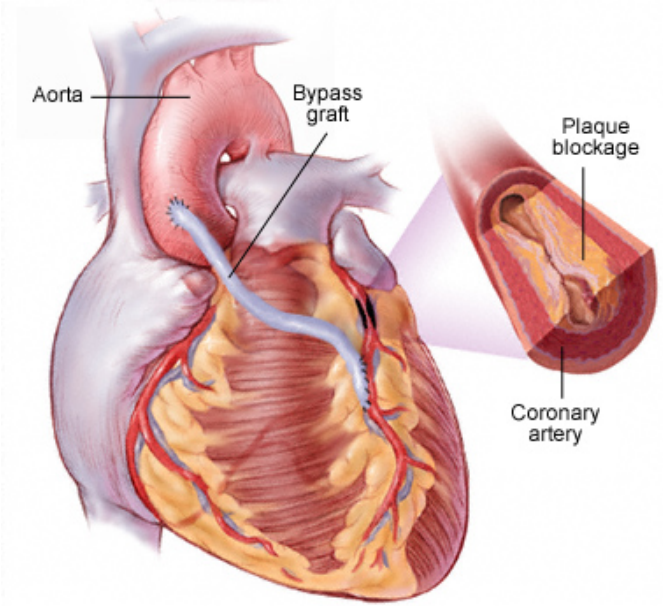

Example 3: Approximation Details

Shape sensitivity

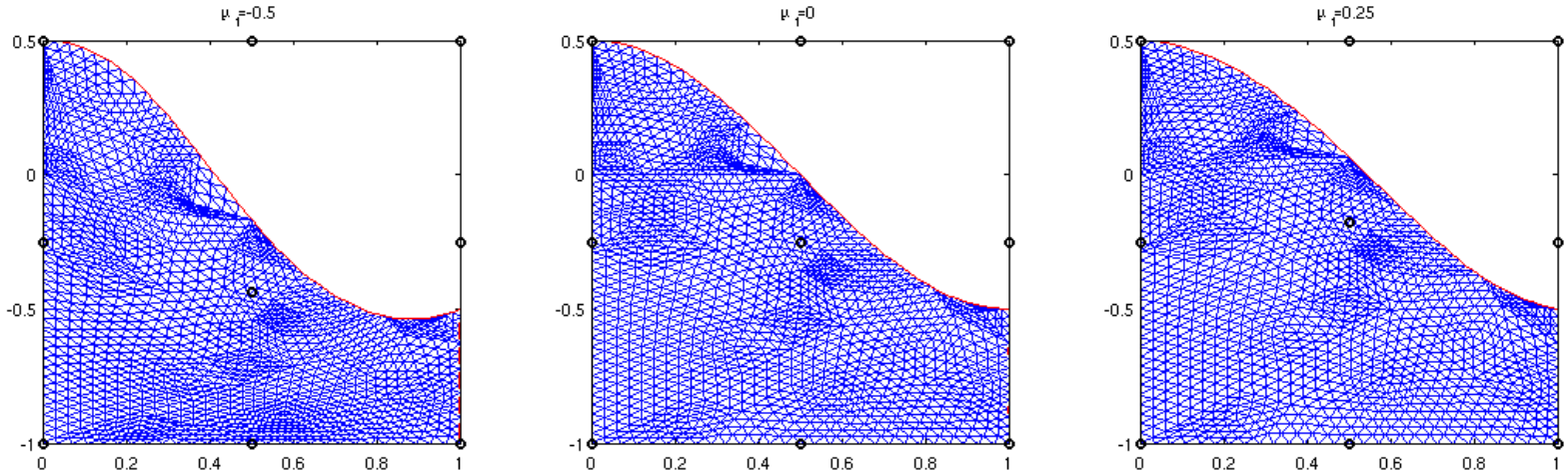

Bypass central sections obtained with FFD for different parameter choices

Number of mesh nodes $\mathcal{N}$	5421
Lattice of FFD control points $\boldsymbol{P}_{i,j}$	3×3
Number of shape parameters*	1
Number of reduced basis functions N †	10
Error tolerance for RB greedy ε_{tol}^{RB}	10^{-4}
Number of affine operator components Q	87
Error tolerance for EIM greedy ε_{tol}^{EIM}	10^{-3}

*Reduction of 100:1 in parametric complexity compared to explicit nodal deformation

†Reduction of 400:1 in linear system dimension

ÉCOLE POLYTECHNIQUE FÉDÉRALE DE LAUSANNE

Example 3: Approximation Details

Shape sensitivity

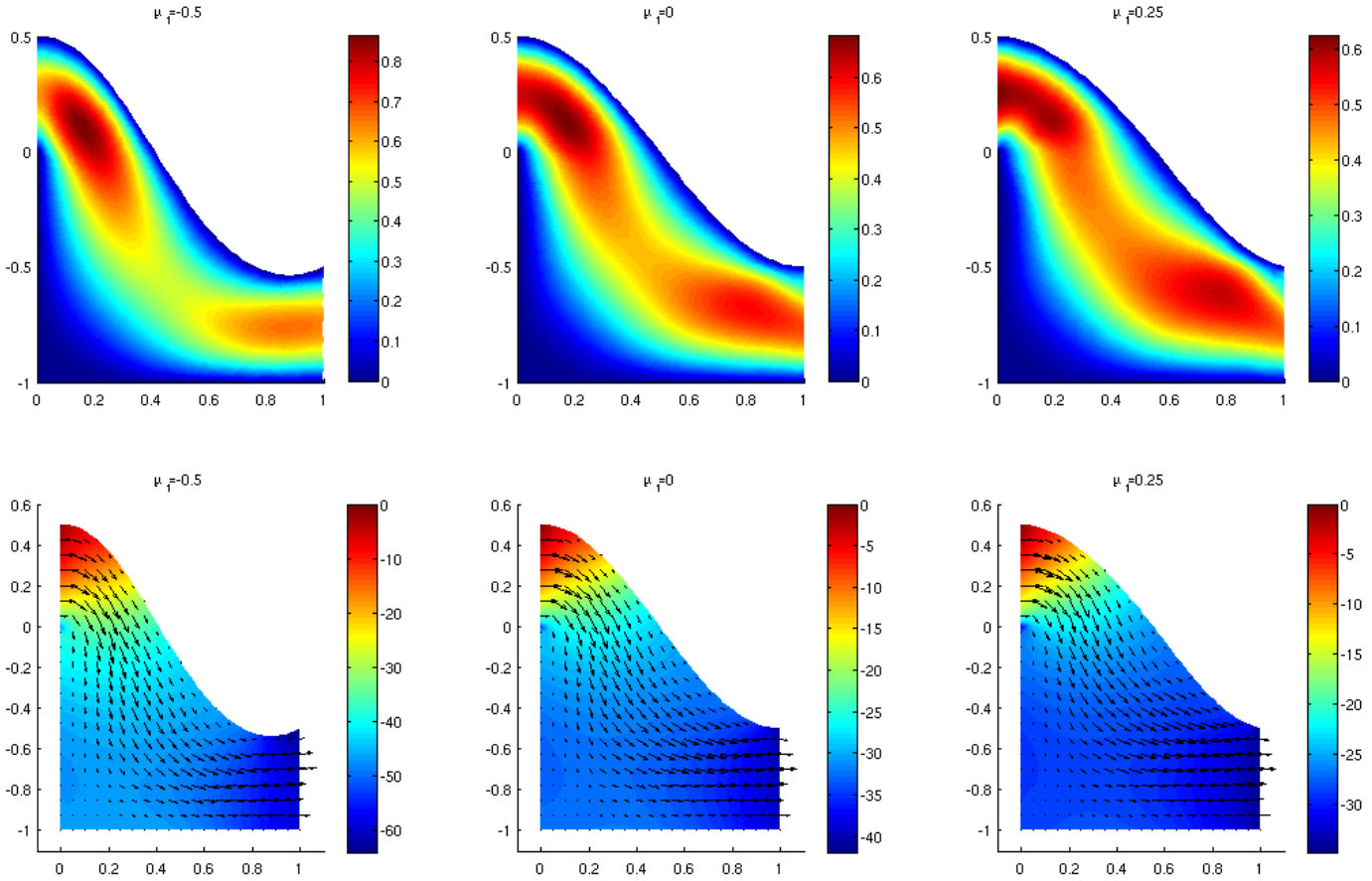

Velocity and pressure fields for different parameters (`rbMIT` + `MLife`)

Example 3: Approximation Details

Shape optimization

$$\min_{\mu \in \mathscr{D}} \quad \frac{\gamma}{2} \int_{\Omega_o^c(\mu)} |\nabla \times \mathbf{u}(\mu)|^2 \, d\Omega_o$$

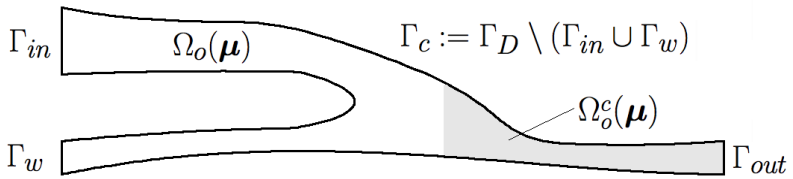

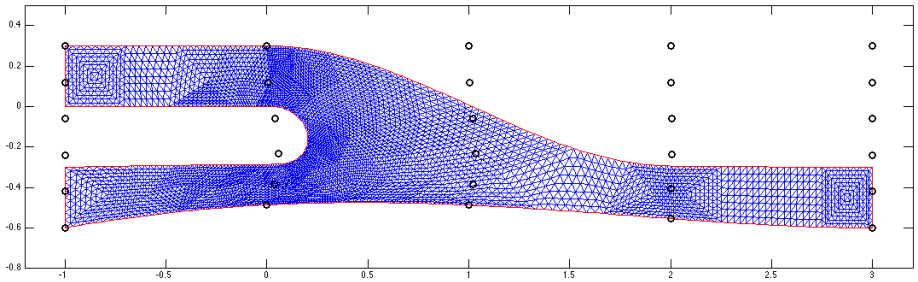

Initial configuration

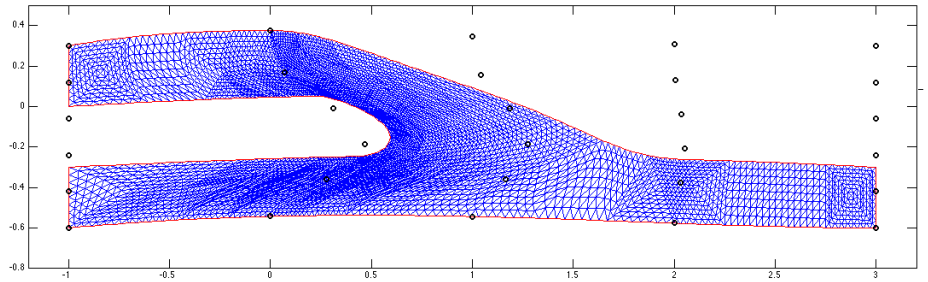

Final configuration

Number of mesh nodes $\mathscr{N}$	4269
Lattice of FFD control points $\boldsymbol{P}_{i,j}$	5×6
Number of shape parameters*	8
Number of reduced basis functions N †	23
Error tolerance for RB greedy ε_{tol}^{RB}	10^{-4}
Number of affine operator components Q	122
Error tolerance for EIM greedy ε_{tol}^{EIM}	10^{-6}

*Reduction of 51:1 in parametric complexity compared to explicit nodal deformation

†Reduction of 540:1 in linear system dimension

ÉCOLE POLYTECHNIQUE FÉDÉRALE DE LAUSANNE

Example 3: Approximation Details

Shape optimization

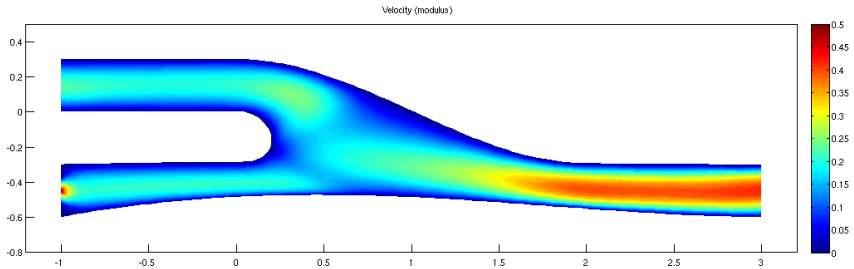

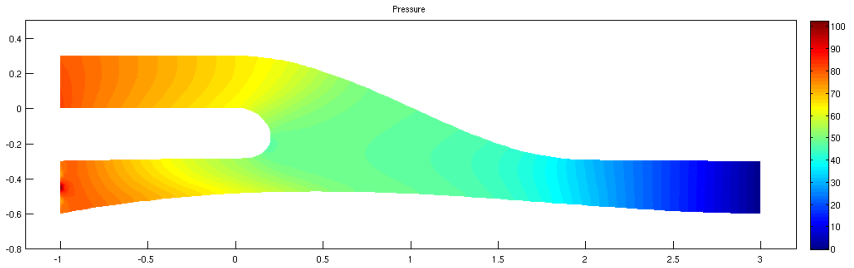

Initial configuration

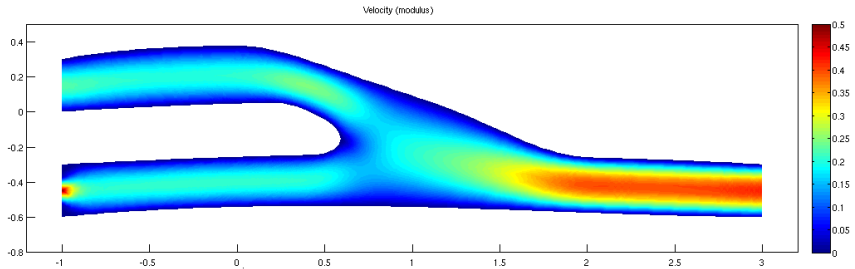

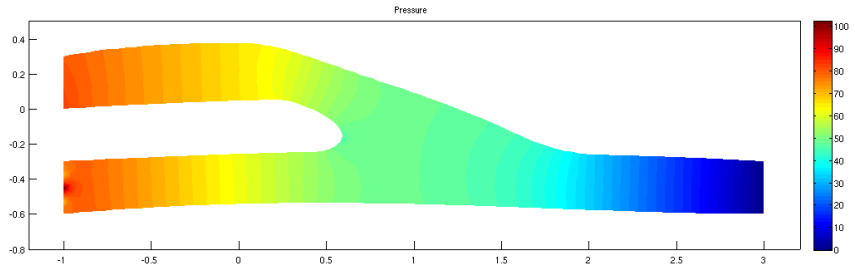

Final configuration

Output evaluations during optimization	45
Vorticity reduction	37%
t_{FE}^{online}	207.21s
t_{RB}^{online}	1.251s
speedup	195

ÉCOLE POLYTECHNIQUE FÉDÉRALE DE LAUSANNE

3D applications in larger contexts

- Applications more oriented to industry and realistic problems (thermal, micro-fluidic, material science and life sciences)
- Large scale problems and complex systems (multiphysics)
- Integration of the metodology into the "HPC" (High-Performance Computing) framework

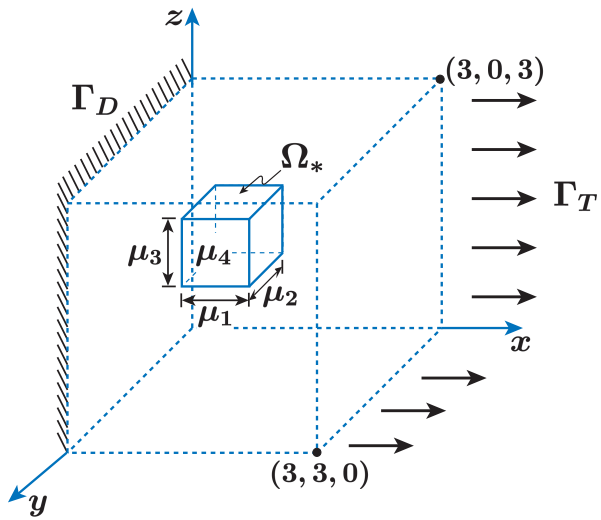

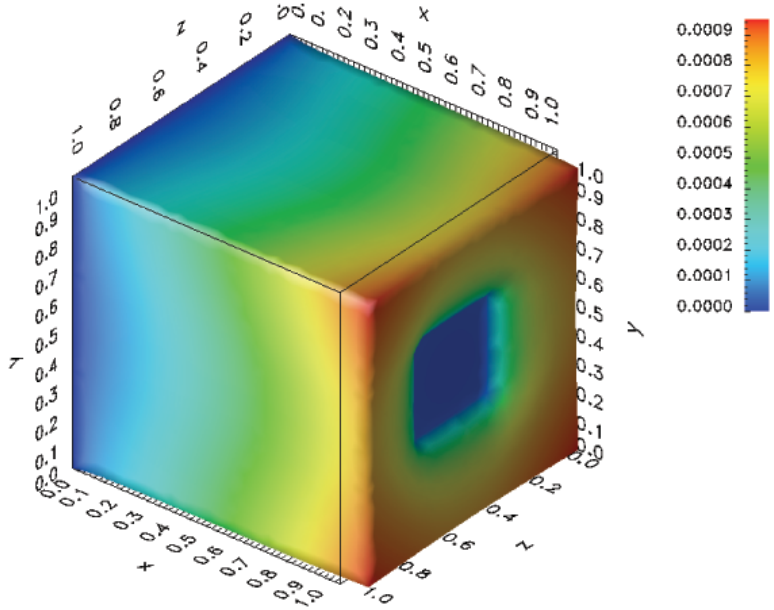

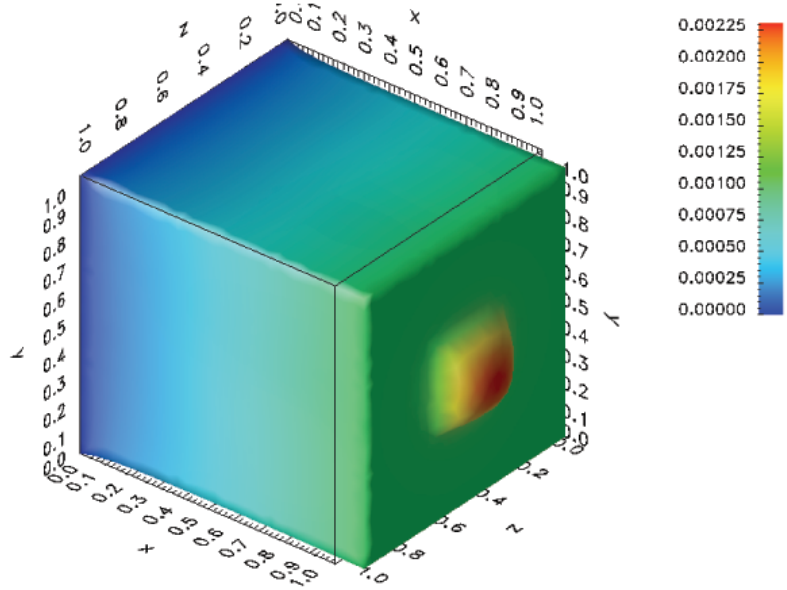

Towards a general approach on free boundary problems

- Fluid-Structure Interaction problems (blood flow in arteries)
- FFD is used to manage the geometrical parameters modelling the wall displacement (structure, elastic part)

Strong parametric coupling FSI

1) Initial guess μ^0, $k = 0$;
2) repeat

   solve the RB equations for $(\mathbf{u}^k, p^k)$ in $\Omega(\mu^k)$;

   compute assumed traction $\hat{\tau}(\mathbf{u}^k, p^k)$;

   solve the minimization problem

$$\mu^{k+1} = \arg\min_{\mu \in \mathcal{D}} \frac{1}{2} \int_\Sigma |\eta(\mu) - \hat{\eta}|^2 d\Gamma$$

   where $\eta(\mu)$ is the interface displacement given by geometrical parametrization and $\hat{\eta}$ solves

$$\int_\Sigma K \hat{\eta}' \beta' d\Gamma = \int_\Sigma \hat{\tau} \beta d\Gamma \quad \forall\, \beta \in X(\Sigma);$$

   k := k+1;

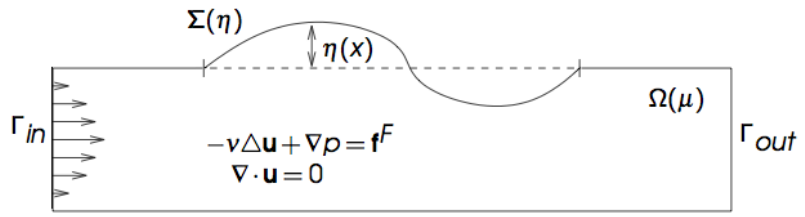

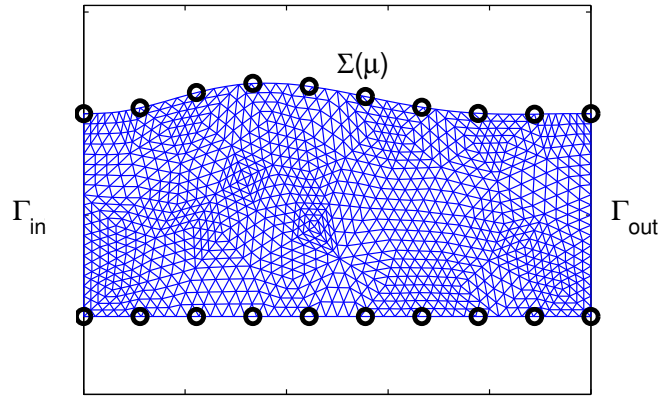

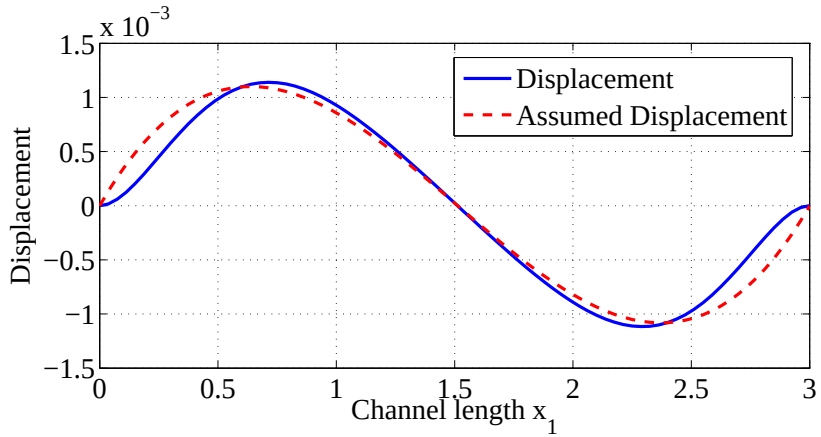

Summary

Optimal control...

- Suitable shape parametrizations enable to use optimal control theory
- Flexible approach providing powerful tools for solving different problems

...and reduced modelling...

- Model order reduction by geometrical parametrization and PDE solved with reduced basis methods
- Free-form deformations are a flexible shape parametrization tool which can be coupled with reduced basis methods

... for complex problems

- Interest in working with (linear/nonlinear) viscous flows in more realistic geometries
- Possibility to provide rapid and reliable optimal solutions

References

DR09 **S. Deparis and G. Rozza**. Reduced basis method for multi-parameter dependent steady NavierStokes equations: applications to natural convection in a cavity. Journal of Computational Physics, 228: 4359–4378, 2009.

GP05 **M. Grepl and A.T. Patera**. *A posteriori error bounds for reduced-basis approximations of parametrized parabolic partial differential equations*. ESAIM: Math. Model. Numer. Anal., 39(1):157–181, 2005.

HNRP09 **N.C. Nguyen, G. Rozza, D. Huynh and A.T. Patera**. *Reduced basis approximation and a posteriori error estimation for parametrized parabolic PDEs; Application to real-time Bayesian parameter estimation*. In Biegler, Biros, Ghattas, Heinkenschloss, Keyes, Mallick, Tenorio, van Bloemen Waanders, & Willcox (Eds), 2009, Computational Methods for Large Scale Inverse Problems and Uncertainty Quantification, John Wiley & Sons, UK (revised/submitted).

LR09 **T. Lassila and G. Rozza**. *Parametric free-form shape design with PDE models and reduced basis method*. Comput. Methods Appl. Mech. Engrg., submitted, 2009.

LMR06 **A.E. Lovgren, Y. Maday and E.M. Ronquist**. *The reduced basis element method for fluid flows. Advances in Mathematical Fluid Mechanics*, 129–154. Birkhauser, Basel, 2006.

NRP09 **N.C. Nguyen, G. Rozza and A.T. Patera**. *Reduced Basis Approximation and A Posteriori Error Estimation for the Time- Dependent Viscous Burgers Equation*. Calcolo, 46: 157–185, 2009.

PR07 **A.T. Patera and G. Rozza**. Reduced Basis Approximation and A Posteriori Error Estimation for Parametrized Partial Differential Equations. Version 1.0, Copyright MIT 2006, to appear in (tentative rubric) MIT Pappalardo Graduate Monographs in Mechanical Engineering, available at `http://augustine.mit.edu`.

QR03 **A, Quarteroni and G. Rozza**. *Optimal control and shape optimization of aorto-coronaric bypass anastomoses*. M^3AS 13 (12), 1801–1823, 2003.

ÉCOLE POLYTECHNIQUE FÉDÉRALE DE LAUSANNE

References

QR07 **A. Quarteroni and G. Rozza**. *Numerical solution of parametrized Navier-Stokes equations by reduced basis methods*. Numer. Methods Partial Differential Equations, 23(4): 923–948, 2007.

R05 **G. Rozza**. *Shape design by optimal flow control and reduced basis techniques: applications to bypass configurations in haemodynamics*. PhD Thesis No. 3400, EPFL, 2005.

R09a **G. Rozza**. *Reduced Basis Methods for Stokes Equations in domains with non affine parameter dependence*. Computing and Visualization in Science, Vol. 12, No. 1: 23–35, 2009.

R09b **G. Rozza**. *Reduced Basis approximation and error bounds for potential flows in parametrized geometries*. Submitted, 2009.

RHP08 **G. Rozza, D.B.P. Huynh, and A.T. Patera**. *Reduced basis approximation and a posteriori error estimation for affinely parametrized elliptic coercive partial differential equations*. Arch. Comput. Methods Engrg.,15: 229–275, 2008.

RHSP07 **G. Rozza, D.B.P. Huynh, S. Sen, A.T. Patera**. *A Successive Constraint Linear Optimization Method for Lower Bounds of Parametric Coercivity and Inf-Sup Stability Constants*. C.R. Acad. Sci. Paris, Ser. I 345: 473–478, 2007.

RNPD09 **G. Rozza, N.C. Nguyen, A.T. Patera and S. Deparis**. *Reduced Basis Methods and a posteriori error estimators for heat transfer problems*. HT2009-88211 Proceedings of HT2009 2009 ASME Summer Heat Transfer Conference, July 19-23, 2009, San Francisco, California, USA.

RV07 **G. Rozza and K. Veroy**. *On the stability of the reduced basis method for Stokes equations in parametrized domains*. Comput. Methods Appl. Mech. Engrg., 196(7):1244–1260, 2007.

SP86 **T.W. Sederberg and S.R. Parry**. *Free-form deformation of solid geometric models*. Comput. Graph., 20(4), 1986.

ÉCOLE POLYTECHNIQUE FÉDÉRALE DE LAUSANNE